Biogeosciences, 9, 249–268, 2012
www.biogeosciences.net/9/249/2012/
doi:10.5194/bg-9-249-2012

Biogeosciences

Spatial and temporal CO_2 exchanges measured by Eddy Covariance over a temperate intertidal flat and their relationships to net ecosystem production

P. Polsenaere[1,*], E. Lamaud[2], V. Lafon[1], J.-M. Bonnefond[2], P. Bretel[1], B. Delille[1,3], J. Deborde[1,4], D. Loustau[2], and G. Abril[1,5]

[1]Laboratoire Environnements et Paléoenvironnements OCéanique (EPOC), Université Bordeaux 1, CNRS-UMR5805, Avenue des Facultés, 33405 Talence Cedex, France
[2]Laboratoire Ecologie fonctionnelle et PHYSique de l'Environnement (EPHYSE), INRA, Centre de Bordeaux-Aquitaine, 71 Avenue Edouard Bourlaux, 33883 Villenave d'Ornon Cedex, France
[3]Unité Océanographie Chimique, Département d'Astrophysique, Géophysique et Océanographie, Université de Liège, Allée du 6 Août, 17-Bât. B5 4000 Liège, Belgium
[4]Institut de Recherche pour le Développement (IRD), 101 Promenade Roger Laroque-Anse Vata BPA5 98848 Nouméa, Nouvelle-Calédonie, France
[5]Institut de Recherche pour le Développement (IRD), Laboratorio de Potamologia Amazônica, LAPA, Universidade Federal do Amazônas, Manaus, Brazil
[*]present address: Royal Netherlands Institute for Sea Research (NIOZ), Ecosystem Studies Department, Korringaweg 7, 4401 NT Yerseke, The Netherlands

Correspondence to: P. Polsenaere (p.polsenaere@nioo.knaw.nl, p.polsenaere@epoc.u-bordeaux1.fr)

Received: 23 May 2011 – Published in Biogeosciences Discuss.: 6 June 2011
Revised: 4 December 2011 – Accepted: 26 December 2011 – Published: 12 January 2012

Abstract. Measurements of carbon dioxide fluxes were performed over a temperate intertidal mudflat in southwestern France using the micrometeorological Eddy Covariance (EC) technique. EC measurements were carried out in two contrasting sites of the Arcachon flat during four periods and in three different seasons (autumn 2007, summer 2008, autumn 2008 and spring 2009). In addition, satellite images of the tidal flat at low tide were used to link the net ecosystem CO_2 exchange (NEE) with the occupation of the mudflat by primary producers, particularly by *Zostera noltii* meadows. CO_2 fluxes during the four deployments showed important spatial and temporal variations, with the flat rapidly shifting from sink to source with the tide. Absolute CO_2 fluxes showed generally small negative (influx) and positive (efflux) values, with larger values up to $-13\,\mu mol\,m^{-2}\,s^{-1}$ for influxes and $19\,\mu mol\,m^{-2}\,s^{-1}$ for effluxes. Low tide during the day was mostly associated with a net uptake of atmospheric CO_2. In contrast, during immersion and during low tide at night, CO_2 fluxes where positive, negative or close to zero, depending on the season and the site. During the autumn of 2007, at the innermost station with a patchy *Zostera noltii* bed (cover of $22 \pm 14\,\%$ in the wind direction of measurements), CO_2 influx was $-1.7 \pm 1.7\,\mu mol\,m^{-2}\,s^{-1}$ at low tide during the day, and the efflux was $2.7 \pm 3.7\,\mu mol\,m^{-2}\,s^{-1}$ at low tide during the night. A gross primary production (GPP) of $4.4 \pm 4.1\,\mu mol\,m^{-2}\,s^{-1}$ during emersion could be attributed to microphytobenthic communities. During the summer and autumn of 2008, at the central station with a dense eelgrass bed ($92 \pm 10\,\%$), CO_2 uptakes at low tide during the day were -1.5 ± 1.2 and $-0.9 \pm 1.7\,\mu mol\,m^{-2}\,s^{-1}$, respectively. Night time effluxes of CO_2 were 1.0 ± 0.9 and $0.2 \pm 1.1\,\mu mol\,m^{-2}\,s^{-1}$ in summer and autumn, respectively, resulting in a GPP during emersion of 2.5 ± 1.5 and $1.1 \pm 2.0\,\mu mol\,m^{-2}\,s^{-1}$, respectively, attributed primarily to the seagrass community. At the same station in April 2009, before *Zostera noltii* started to grow, the CO_2 uptake at low tide during the day was the highest ($-2.7 \pm 2.0\,\mu mol\,m^{-2}\,s^{-1}$). Influxes of CO_2 were also observed during immersion at the central station in spring and early autumn and were apparently related to phytoplankton blooms occurring at the mouth of the flat, followed by the advection of CO_2-depleted water with the flooding tide.

Although winter data as well as water carbon measurements would be necessary to determine a precise CO_2 budget for the flat, our results suggest that tidal flat ecosystems are a modest contributor to the CO_2 budget of the coastal ocean.

1 Introduction

The coastal zone is defined as the ocean area on the continental shelf with a depth of less than 200 m, including all estuarine areas to the upstream limit of tidal influence. The coastal zone receives considerable amounts of nutrients and organic matter from the land, exchanges matter and energy with the open ocean (Borges, 2005) and thus constitutes one of the most biogeochemically active areas of the biosphere (Gattuso et al., 1998; Borges et al., 2005). In the coastal ocean, shallow depth favours light penetration in a large part of the water column and allows for a strong coupling between pelagic and benthic processes. These characteristics make the coastal zone very active in terms of CO_2 exchange with atmosphere, benthic and pelagic primary production and respiration (Gazeau et al., 2004; Borges et al., 2006). The coastal zone covers approximately 7 % of the surface of the global ocean; despite its relatively modest surface area, this zone accounts for 14–30 % of all oceanic primary production, 80 % of organic matter burial and 90 % of sedimentary mineralisation (Mantoura et al., 1991; Pernetta and Milliman, 1995). In addition, continental shelves act as a net sink of CO_2 of $-0.21 \pm 0.36\,\mathrm{PgC\,yr^{-1}}$ – i.e. 15 % of the open ocean sink – whereas near-shore estuarine environments emit to the atmosphere $+0.27 \pm 0.23\,\mathrm{PgC\,yr^{-1}}$ (Laruelle et al., 2010). This active but heterogeneous region of the ocean has recently begun to be taken into account in global carbon budgeting efforts (Frankignoulle et al., 1998; Borges, 2005).

The ability of an ecosystem to consume CO_2 and produce organic matter is governed to a large extent by its net ecosystem production (NEP), defined either as the rate of net organic carbon burial and export or as the difference between ecosystem-level gross primary production (GPP) and community respiration (CR) (Smith and Hollibaugh, 1993; Gattuso et al., 1998). GPP represents the C fixation by autotrophic organisms, and CR represents the respiration of all organisms, both autotrophic and heterotrophic. Both GPP and CR are summed per unit ground or water area over time (Chapin et al., 2006). Autotrophic ecosystems have GPP greater than their CR and are net producers of organic C that can be accumulated in the system or exported outside of the system. Heterotrophic ecosystems have GPP lower than their CR and are net consumers of organic C supplied by an external source (Odum, 1956). GPP and CR are processes that also consume and release, on a short timescale, inorganic C in an ecosystem. In a terrestrial system, GPP directly consumes atmospheric CO_2, and CR releases CO_2 directly to the atmosphere. Thus, the net ecosystem exchange (NEE), defined as the net vertical CO_2 exchange between the ecosystem and the atmosphere, is generally approximated by NEP in many terrestrial ecosystems over short timescales (Baldocchi, 2003). In contrast, in aquatic systems, GPP consumes dissolved inorganic carbon and reduces the concentration of CO_2 in the water. This reduction of CO_2 generates a diffusion gradient that causes CO_2 to enter the water from the atmosphere (Chapin et al., 2006). CR in aquatic systems releases CO_2 to the water, where it dissociates into bicarbonate and carbonate ions, generating a water–air CO_2 gradient that tends to emit CO_2 to the atmosphere. Because water–air diffusion is a slow process in comparison with GPP and CR and also compared to lateral water movements, NEE and NEP can be very different over short timescales in aquatic systems (Gattuso et al., 1998; Borges et al., 2006). For instance, a system that receives large amounts of CO_2-saturated water can be autotrophic but also a source of atmospheric CO_2. In addition, a system that receives large amounts of allochthonous organic matter can be heterotrophic but serve as a sink of atmospheric CO_2 if waters are strongly stratified and if the surface layer in contact with the atmosphere becomes net autotrophic. Finally, in aquatic systems, carbonate precipitation and dissolution are additional processes that affect CO_2 concentration; the precipitation of calcium carbonate results in the sequestering of carbon (and a DIC decrease) but is accompanied by a shift of pH that results in the release of CO_2 (Ware et al., 1991). For instance, a significant release of CO_2 to waters as a result of carbonate precipitation by invasive benthic macrofauna has been reported in San Francisco Bay (Chauvaud et al., 2003). Inversely, a significant reduction of CO_2 degassing resulting from carbonate dissolution has been reported in a turbid, eutrophic and heterotrophic estuary (Abril et al., 2003).

In the coastal zone, NEP and GPP show important variations both spatially and temporally, depending on a large suite of environmental factors, mainly light and nutrient availability and organic matter loads. Open shelves are net autotrophic and serve as CO_2 sinks (Gazeau et al., 2004; Borges, 2005). Estuaries are generally heterotrophic and are a CO_2 source because of the large inputs of labile organic matter from rivers that fuel CR, while GPP is limited in estuaries by light availability (Smith and Hollibaugh, 1993; Frankignoulle et al., 1998; Wang and Cai, 2004; Borges, 2005). Shallow coastal environments colonised with seagrass meadows are generally net autotrophic, with a GPP estimated at $2.7 \pm 0.1\,\mathrm{g\,C\,m^{-2}\,d^{-1}}$ (Duarte et al., 2010). The intertidal area of the coastal zone also has particular properties with respect to NEP and CO_2 fluxes. First, benthic GPP can be greatly enhanced at low tide because of the increased availability of light and high temperature (Parsons et al., 1984; Hubas et al., 2006). During emersion, benthic NEP is equivalent to NEE. However, during immersion, planktonic and benthic NEP do not necessary correspond to NEE, as a substantial advection of metabolic carbon can occur. Indeed,

outwelling of CO_2 supersaturated waters with the tide have been described in salt marsh and mangrove ecosystems (Cai and Wang, 1998; Borges et al., 2003; Wang and Cai, 2004).

CO_2 fluxes at the water–air interface can be measured directly using floating chambers (Frankignoulle et al., 1998) or calculated from water partial pressure of CO_2 (pCO_2) measurements and a given gas transfer velocity. However, CO_2 flux computations can be subject to large uncertainties because of the difficulty in accurately assessing the gas transfer velocity (Raymond and Cole, 2001; Vachon et al., 2010). Similarly, the floating chamber method has been suspected to artificially enhance the CO_2 exchange across the air–water interface (Raymond and Cole, 2001). CO_2 fluxes at the air-sediment interface at low tide can be assessed by deploying benthic chambers (Migné et al., 2002), but this method suffers from variability of intertidal sediment habitat resulting from patchiness at all timescales and particularly from spatial patchiness (Migné et al., 2004). Micrometeorological measurements, especially the Eddy Covariance technique (EC), show potential, as CO_2 fluxes across heterogeneous intertidal areas can be obtained with the same technique, at high tide and low tide (Houghton and Woodwell, 1980; Kathilankal et al., 2008; Zemmelink et al., 2009). In addition, the EC method is non-invasive and provides direct and continuous measurements of the net carbon dioxide exchange of a whole ecosystem across a spectrum of time scales from hours to years (Baldocchi et al., 1988; Aubinet et al., 2000; Baldocchi, 2003). Applying the EC in the coastal zone appears to be a very promising technique, as the method can provide flux data on timescales short enough to resolve the temporal variability induced by the tidal, diurnal and seasonal cycles. However, the method can also have limitations and requires important qualitative and quantitative analyses and corrections because of its physical and theoretical background (Baldocchi et al., 1988). In intertidal ecosystems, EC measurements present the great advantage of providing precise CO_2 fluxes at the air/water interface during immersion and at the air/sediment interface during emersion. In salt marshes, the EC technique has shown substantial changes in fluxes throughout the tidal cycle (Houghton and Woodwell, 1980; Kathilankal et al., 2008). Likewise, Zemmelink et al. (2009) used the EC technique over the intertidal Wadden Sea mudflat in Europe and observed a CO_2 sink, particularly at low tide and during the day.

On four occasions between 2007 and 2009, we employed an EC system in a flat dominated by an intertidal mudflat in southwestern France. Here we present results on the continuous CO_2 fluxes obtained during four different periods over two intertidal areas of the Arcachon flat. The main focuses of this paper are (1) to describe and characterise the temporal and spatial variations of CO_2 exchanges occurring in the flat during the day and night and during emersion and immersion; (2) to understand the CO_2 flux dynamic in relation to the components of NEP (benthic and planktonic GPP and CR) – we focus more specifically on the low tide/day case, during which we could relate CO_2 fluxes to the tidal flat occupation by *Zostera noltii* eelgrass meadows; and (3) to improve present conceptualization of carbon flows through tidal flats and the potential role of these ecosystems in the carbon budget of the coastal ocean.

2 Materials and methods

2.1 Study site

The Arcachon bay is a temperate intertidal flat of 174 km^2 on the southwestern Atlantic coast of France (44°40′ N, 01°10′ W). This triangle-shaped bay is enclosed by the coastal plain of Landes Gascony, and communicates with the Atlantic Ocean through a narrow channel 8 km in length (Fig. 1). With a mean depth of 4.6 m, this shallow flat presents semi-diurnal tides with amplitudes varying from 0.8 to 4.6 m (Plus et al., 2008). During a tidal cycle, the flat exchanges approximately 264×10^6 m^3 and 492×10^6 m^3 of water with the ocean during average neap and spring tides, respectively. The flat also receives freshwater, but to a lesser extent, with an annual input of 1.25×10^9 m^3 (1.8×10^6 m^3 at each tidal cycle), of which 8 % is from groundwater, 13 % is from rainfall and 79 % is from rivers and small streams (Rimmelin et al., 1998). Water temperatures in the bay vary from 6 °C in winter to 22.5 °C in summer, and water salinity varies from 22 to 35 PSU according to freshwater input variations during the year.

The Arcachon flat surface is composed of 57 km^2 of channels, with a maximum depth of 25 m, which drain a large muddy tidal flat of 117 km^2. *Zostera noltii* seagrass beds are particularly extensive and colonise the major part of this intertidal area (60 %, i.e. 70 km^2) between −1.9 m and +0.8 m relative to local Mean Sea Level (Amanieu, 1967). With a net primary production estimated between 45 and 75 Mt C yr^{-1} (I. Auby, personal communication, 2011), the flat is considered as the most important eelgrass meadow of Europe. The microphytobenthic communities also represent a significant proportion of benthic production, which is estimated at between 16 and 18 Mt C yr^{-1}. Together, these two categories of benthic primary production represent more than half of the total primary production of the flat (Auby, 1991). *Zostera noltii* shows contrasted temporal variations in the Arcachon flat. Indeed, the root system growth begins at the end of the winter and maximum amounts of below-ground biomass are achieved in the spring. To the contrary, the leaf growth period begins later in the spring, and leaves reach maximum above-ground biomass in the summer (Auby and Labourg, 1996).

An EC measurement system was then deployed on four occasions and during the spring, summer and autumn seasons at two different intertidal sites of the mudflat (Fig. 1). A first deployment was made in the inner part of the flat at Station 2 characterized by a low *Zostera noltii* seagrass

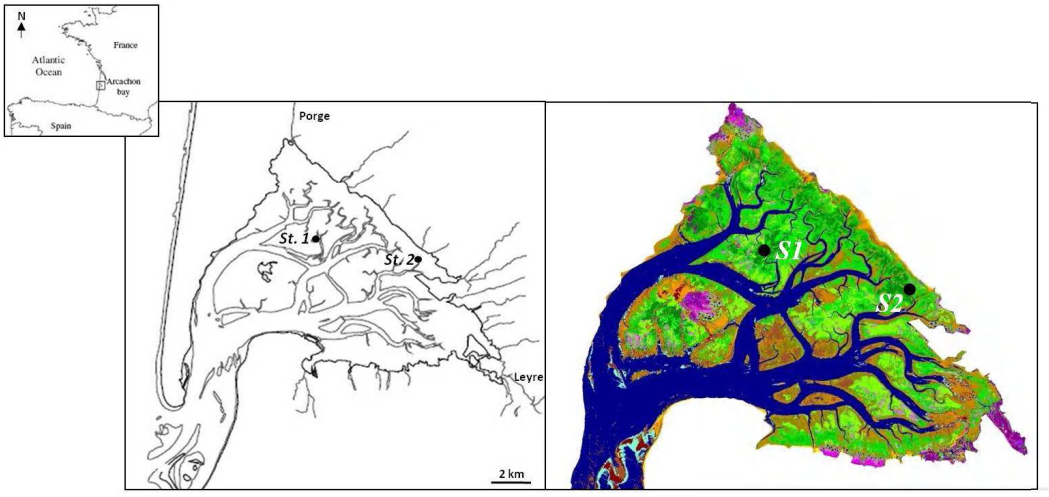

Fig. 1. Localisation of the Eddy Covariance (EC) experimental sites. **(A)** The Arcachon flat with the subtidal zone (channels) and the intertidal mudflat area; **(B)** the two EC sites: Station 1 (44°42′59.15″ N, 01°08′36.96″ W) and Station 2 (44°42′19.96″ N, 01°04′01.35″ W). The *Zostera noltii* seagrass meadow is derived from the SPOT satellite image of the 22 June 2005; it represents 60 % of the intertidal area (shades of green show the differences in seagrass density).

meadow (N 44°42′19.96″, W 01°04′01.35″) in autumn 2007. The three other deployments were carried out in the central part of the flat at Station 1 characterised by a dense eelgrass bed (N 44°42′59.15″, W 01°08′36.96″) in summer 2008, autumn 2008 and spring 2009. During the four experiments, throughout the tidal cycle, the tidal flat was emerged for approximately four hours and immersed for approximately nine hours.

2.2 CO_2 fluxes measured by EC in the Arcachon flat

2.2.1 Theory behind the EC technique

The atmosphere contains turbulence (eddies) caused by buoyancy and shear (Aubinet et al., 2000) of upward and downward moving air that transports trace gases such as CO_2 (Baldocchi, 2003). The EC technique allows for the measurement of these turbulent eddies to determine the net flux of any scalar movement vertically across the ecosystem/atmosphere interface.

The mean turbulent flux of the scalar x in the vertical direction (F_x) is expressed as the covariance between the fluctuations in the vertical wind velocity (w) and the scalar density or concentration (ρ_x) (Moncrieff et al., 1997) as

$$F_x = \overline{w' \rho_x'} \quad (1)$$

where the overbar represents a temporal average (i.e. 10 min were used in the case of the Arcachon flat), and primes denote the instantaneous turbulent fluctuations relative to their temporal average (e.g. $w' = w - \overline{w}$ and $\rho_x' = \rho_x - \overline{\rho_x}$, Reynolds, 1895).

Carbon dioxide fluxes (F_c) can be then defined as

$$F_c = \overline{w' c'} \quad (2)$$

where F_c is expressed in $\mu mol\, m^{-2}\, s^{-1}$, w is expressed in $m\, s^{-1}$ and c (the CO_2 concentration) in $\mu mol\, m^{-3}$. CO_2 fluxes are directed upward when F_c values are positive and downward when corresponding values are negative.

2.2.2 Turbulent flux measurement system in the Arcachon flat

Fluxes of CO_2 were measured using an EC system deployed from 30 September at 11:35 to October 2007 at 08:55 (GMT) at Station 2 (Fig. 1); from the 1 July at 16:40 to 7 July 2008 at 04:00 (GMT); from 25 September at 15:10 to 17 October 2008 at 01:10 (GMT) and from the 1 April at 16:30 to 13 April 2009 at 22:50 (GMT) at Station 1, for a total of 4, 7, 20 and 13 days, respectively.

Our EC system (Fig. 2) was fixed to a mast and consisted of a sonic anemometer (model *CSAT3, Campbell Scientific Inc.*, Logan, UT) to measure the three wind speed components ($m\, s^{-1}$), as well as the sonic temperature (°C), and an infra-red gas analyser (model *LI-7500, Licor Inc.*, Lincoln, NE) that measured CO_2 and H_2O concentrations ($mmol\, m^{-3}$) and atmospheric pressure (kPa). Analogue output signals from these fast-response instruments were sampled and digitised at the rate of 20 Hz. With these two main EC sensors separated by a distance of 0.25 m, a filtered silicon quantum sensor (*SKP215, Skye Instruments*, Llandrindod Wells, UK) was used to measure photosynthetically active radiation (PAR, $\mu mol\, m^{-2}\, s^{-1}$) every minute

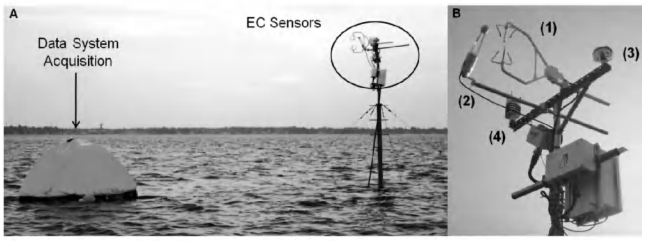

Fig. 2. The Eddy Covariance system deployed in the Arcachon flat in April 2009. **(A)** General view of the system measurement showing the sensors mounted on the mast and the data system acquisition *Campbell CR3000* in the lifeboat; **(B)** the sensors: (1) the sonic anemometer *CSAT3*, (2) the infra-red gas analyser *LI-7500*, (3) the quantum sensor *SKP215* and (4) the meteorological station (*Vaisala WXT510*). The measurement heights were 4.20, 5.50, 7.0 and 5.0 m in September–October 2007, July 2008, September–October 2008 and April 2009, respectively.

(Fig. 2b). Additionally, a meteorological transmitter (model *WXT510, Vaisala Inc.*, Finland) was set up in September–October 2008 and April 2009. This transmitter provided additional wind speed and direction measurements that could be compared with data from the sonic anemometer and other weather parameters: air temperature, pressure, humidity, and the amount, intensity and duration of rainfall events. The sensors were mounted on a mast inserted in the mud and secured by three wires to keep it vertical and to limit vibrations that could bias EC flux measurements (Fig. 2a). Data were recorded by a central acquisition system (model *CR3000, Campbell Scientific Inc.*, Logan, UT) (connected to the sensors with a waterproof cable) located in an anchored inflatable raft and protected by a tide pool. The entire system was powered by rechargeable lead batteries (12 volts, 100 amperes per hour) and those latter were replaced every four days.

The equipment used was similar for the four deployments except during September–October 2007, when a different sonic anemometer (model *Windmaster, Gill Instr.*, UK) was used, as well as a different sample frequency for both EC sensors, i.e. 10 Hz. Also during this deployment, the PAR was not directly measured at the EC station but at the Cap Ferret meteorological station (N 44°37′54″, W 01°14′54″, 14 km from Station 2). Global radiation ($J\,cm^{-2}$) hourly data were first obtained and then converted to $W\,m^{-2}$ and to $\mu mol\,m^{-2}\,s^{-1}$, assuming a factor of 2 from $W\,m^{-2}$ to $\mu mol\,m^{-2}\,s^{-1}$, to homogenise PAR units between the four deployments. The sensors for the four field setups were mounted at maximum heights (during low tide) of 4.20, 5.50, 7.0 and 5.0 m in September–October 2007, July 2008, September–October 2008 and April 2009, respectively.

2.2.3 Data processing and quality control

Raw data were processed following the Aubinet et al. (2000) methodology developed in the context of the EUROFLUX project for net carbon and water exchanges of forests and modified to be applied to intertidal areas. The first important adaptation of the forest-based methodology to the case of the Arcachon mudflat was to adjust for variations in the relative measurement height with the tidal rhythms, which must be included in EC data computations and corrections. Secondly, fluxes were computed with a shorter averaging period (10 min) than usually used (30 min) to detect the quick transitions from low tide to high tide and vice versa. Data were processed using the EdiRe software from the University of Edinburg (Scotland) by applying the following steps: (1) spike removal in anemometer or gas analyser data; (2) unit modifications and statistical operations; (3) coordinating rotation to align coordinate system with the stream lines of the 10 min. averages; (4) linear de-trending of sonic temperature, H_2O and CO_2 channels; (5) determining time lag values for H_2O and CO_2 channels using a cross-correlation procedure; (6) computing mean values, turbulent fluxes and characteristic parameters, e.g. the Monin–Obhukov stability index Z/L; (7) high-frequency corrections via transfer functions based on Kaimal–Moore's co-spectral models (Kaimal et al., 1972; Moore, 1986); and (8) performing a Webb-Pearman-Leuning correction to account for the effects of fluctuations of temperature and water vapour on measured fluctuations in CO_2 and H_2O (Webb et al., 1980). In parallel to frequency corrections, a cospectral analysis was carried out for each period to quantify the distribution by frequency of the covariance of the raw measured signals.

According to data quality control protocols, incorrect processed data must be removed to obtain reliable CO_2 flux measurements. Several factors can lead to bias or errors, i.e. instrument malfunctions, processing/mathematical artefacts, ambient conditions not satisfying the EC methodology (non-stationary periods, convergence, divergence), heavy precipitation – particularly for open-path gas analyser – or a measurement footprint larger than the fetch of interest (Burba and Anderson, 2005). Two main statistical tests were used: (1) the steady-state test was applied to pairs of specified signals, particularly to w and c in this study. Standard deviations and covariances of w and c were computed on short time intervals of 1 min, and these values were compared to those computed on the chosen time run of 10 min, following Foken and Wichura (1996). Only data corresponding to a difference lower than 30 % (periods defined as steady-state conditions) were retained. (2) The statistical test was based on the integral turbulence characteristics of wind components and temperature, according to Foken et al. (1991, 1997). The σ_w/u^* and σ_T/T^*ratios of the data signals (where σ is the standard deviation of the specified signals) were computed and compared to their parameterised values according to different ranges of stability (Z/L parameter). Only data matching

with a difference of less than 50 % were retained. Using these two statistical tests, the retained EC data for the Arcachon flat corresponded to "high-quality data" with a general flag from 1 to 3, according to Foken (2003). In the end, 73 %, 83 %, 83 % and 87 % of CO_2 flux data were retained for the September–October 2007, July 2008, September–October 2008 and April 2009 periods, respectively.

2.3 Eelgrass retrieval from satellite data

The available fetch over homogeneous mudflat always ranged between at least 1000 m at Station 1 and 700 m at Station 2 at low tide in all the wind directions (Fig. 1). Thus, we can assume that all measured fluxes were from the intertidal area of interest, the fetch being generally larger than the footprint of the measurements. Indeed, the relative maximum sensor height at low tide was 4.20 m at Station 2 and ranged between 5 and 7 m at Station 1; it is generally accepted that the relative height:footprint ratio must be 1:100 and 1:300 for unstable and stable atmospheric conditions, respectively (Leclerc and Thurtell, 1990; Hsieh et al., 2000). In the following, we therefore assume that the footprint of our measurement was close to 1 km due to the unstable prevailing atmospheric conditions in the flat and its low surface roughness too.

To relate the temporal and spatial variations in the measured NEE with the distribution of vegetation on the mudflat, satellite images at low tide during the day were analysed. The occupation of the *Zostera noltii* eelgrass meadows was quantified within a circle of 1 km radius centred on the EC mast for both sites. To achieve the most precise resolution of the seagrass cover, each circle was then divided into 32 sectors of 11.25°. Each of them was analysed and according to their relevance, grouped into bigger sectors as: 0–45°: north-northeast, 45–90°: east-northeast, 90–135°: east-southeast, 135–180°: south-southeast, 180–225°: south-southwest, 225–270°: west-southwest, 270–315°: west-northwest and 315–360°: north-northwest wind directions. Satellite images from SPOT were processed using the methodology based on the normalised vegetation index (Barillé et al., 2010). With the exception of the very low eelgrass densities that can be confused with microphytobenthos, the seagrass meadow surfaces can be assessed and the associated cover density can be derived from these images. This approach has been applied to the retrieval of the meadows at Arcachon. For this purpose, images from the CNES/Kalideos database were used. Georeferenced images were downloaded and calibrated using field reflectance data. Finally, channel surfaces, oyster farms, and salt marshes were masked, before calculating the vegetation index on a pixel basis. The eelgrass position and density were deduced from the 2-D mapped index. A dataset of 36 GPS observations collected during autumn 2009 were compared to a SPOT map derived from an image acquired 8 September 2009. The results show that ground-truthing corroborated the map in approximately 90 % of the cases. This test validates this mapping approach that was applied to the five satellite images used in this study.

In total, we analysed five images corresponding to the flat at low tide during the day. The first was recorded on 13 September 2007, precisely matching with the EC deployment carried out in autumn 2007 at Station 2 in the back of the flat. The second image, recorded on 17 October 2008, matched the deployment made in autumn 2008 at Station 1 in the centre of the flat. The third image, recorded at the same station and at the same season the next year, on 8 September 2009, was solely used to evaluate the inter-annual change of the seagrass meadow. Finally, no image precisely matched the deployment from spring 2009 at Station 1, with the closest matching image recorded on 24 June 2009. A fifth image, recorded the next year at Station 1 on 14 April 2010, was also analysed. The latter two images provided insights on the possible changes of the meadow during the spring period.

3 Results

Because diurnal and tidal rhythms largely controlled the CO_2 fluxes, the following results refer to the four distinct cases generated by these two cycles: emersion around low tide during the day (LT/Day), emersion at night (LT/Night), immersion around high tide during the day (HT/Day) and immersion at night (HT/Night). The dynamics of the NEE in relation to the environmental parameters are described for each EC measurement as presented in Table 1 and Figs. 3, 4, 5 and 6.

3.1 Autumn 2007 at Station 2

Over the four days of measurements in September–October 2007 at Station 2, the Arcachon flat acted as a source of CO_2 to the atmosphere, with an average daily flux of $0.5 \pm 0.5\,g\,C\,m^{-2}\,day^{-1}$ and values ranging from 0.1 to $1.0\,g\,C\,m^{-2}\,day^{-1}$ (Table 1) . However, at shorter time scale, strong CO_2 flux variations were observed with flux values ranging from -10 to $19\,\mu mol\,m^{-2}\,s^{-1}$, the flat shifting from sinks to source of CO_2 with both tidal and diurnal rhythms (Table 1, Fig. 3e). At low tide during sunny afternoons with PAR values reaching more than $1000\,\mu mol\,m^{-2}\,s^{-1}$ at midday (Fig. 3a), strong CO_2 uptakes (CO_2 sinks) were systematically observed, as seen on Days 273 and 274, with values close to 6 and $10\,\mu mol\,m^{-2}\,s^{-1}$, respectively (Fig. 3e). In contrast, during night time at low tide, the flat emitted large quantities of CO_2 to the atmosphere, acting as a CO_2 source ($2.7 \pm 3.7\,\mu mol\,m^{-2}\,s^{-1}$ on average, Table 1), as measured between Days 273 and 274 and between Days 275 and 276, with values largely above $10\,\mu mol\,m^{-2}\,s^{-1}$ (Fig. 3e). The CO_2 uptake observed at LT/Day 275 was weak, reaching only $2\,\mu mol\,m^{-2}\,s^{-1}$, compared to that observed on preceding days (Fig. 3e); this change corresponded

Table 1. Carbon dioxide fluxes (F_c) (mean ± standard deviation) measured in the Arcachon flat in September/October 2007 at Station 2 and July 2008, September/October 2008 and April 2009 at Station 1 (see Fig. 1). Negative fluxes represent sinks of CO_2 and positive fluxes represent sources of $CO_2$to the atmosphere by convention. Averaged F_c values have been obtained computing the average over the whole data set for each of the four periods. Daily F_c values represent the average over the averages obtained for every entire days of each period and converted into g C m^{-2} day^{-1} (90 %, 92 %, 97 % and 96 % of data were used, for the deployments in autumn 2007, summer 2008, autumn 2008 and spring 2009 respectively). A PAR threshold of 20 µmol m^{-2} s^{-1} has been chosen to separate day and night cases and high tide cases corresponding to non-zero water heights. * Negative F_c data corresponding to very short periods of low tide/night and very fast changes in CO_2 fluxes in April 2009 (Days 94 and 96, Fig. 6e) were excluded from the average, as they were potentially affected by flooded areas.

F_c (mean ± SD)	Low Tide/Day (µmol m^{-2} s^{-1})	Low Tide/Night (µmol m^{-2} s^{-1})	High Tide/Day (µmol m^{-2} s^{-1})	High Tide/Night (µmol m^{-2} s^{-1})	Average F_c (µmol m^{-2} s^{-1})	Daily F_c (g C m^{-2} day^{-1})
September/October 2007 (Station 2)	−1.7 ± 1.7 (−10.0–0.9)	2.7 ± 3.7 (0.2–18.6)	0.4 ± 1.1 (−2.4–3.9)	1.9 ± 2.4 (−0.4–13.3)	0.8 ± 2.7 (−10.0–18.6)	0.5 ± 0.5 (0.1–1.0)
July 2008 (Station 1)	**−0.3 ± 3.3** (−5.7–12.00)	**0.9 ± 0.8** (−2.5–3.1)	**−0.2 ± 1.4** (−5.0–7.3)	**0.7 ± 1.9** (−2.8–10.6)	**0.1 ± 1.9** (−5.7–12.0)	**0.1 ± 1.0** (−0.7–1.8)
September/October 2008 (Station 1)	**−0.7 ± 2.3** (−10.8–14.3)	**0.2 ± 1.1** (−7.1–5.3)	**−0.1 ± 0.7** (−5.9–3.4)	**−0.3 ± 1.3** (−7.5–4.5)	**−0.2 ± 1.4** (−10.8–14.3)	**−0.2 ± 0.7** (−1.2–1.2)
April 2009 (Station 1)	**−2.7 ± 2.0** (−11.7–0.6)	**−1.3 ± 1.4*** (−6.2–1.9)	**−1.7 ± 1.4** (−8.7–2.6)	**−3.2 ± 2.4** (−13.1–0.4)	**−2.4 ± 2.1** (−13.1–2.6)	**−2.4 ± 0.9** (−4.3–−0.9)

to the occurrence of a mass of relatively hot air (approaching 24 °C, Fig. 3b) concomitant with a change in wind direction from the east-southeast (90–135°) to south-southwest (180–225°) (Fig. 3d) sectors and with a higher speed, above 5 m s^{-1} (Fig. 3c).

3.2 Summer 2008 at Station 1

In July 2008, at Station 1, the Arcachon flat represented a small source of CO_2 to the atmosphere with a mean daily CO_2 flux of 0.1 ± 1.0 g C m^{-2} day^{-1}, shifting from sinks to source of CO_2 from one day to another day (daily flux range: −0.7–1.8 g C m^{-2} day^{-1}, Table 1). With both diurnal and tidal cycles, the flat showed weaker CO_2 exchanges than in autumn 2007 at Station 2 with CO_2 flux values ranging from −6 to 12 µmol m^{-2} s^{-1} (Fig. 4e, Table 1). During summer 2008 at LT/Day, high CO_2 uptakes were measured, reaching values of −5 µmol m^{-2} s^{-1}, as observed during Day 187 (Fig. 4e). These CO_2 sinks occurred particularly during sunny days, with PAR values close to 1500 µmol m^{-2} s^{-1} at midday, and were roughly synchronised with low tides (from Days 185 to 188, Fig. 4a). PAR values measured during this season showed variable but intense radiations above 2000 µmol m^{-2} s^{-1} at midday (Days 185 and 186, Fig. 4a). At LT/Night, CO_2 emissions to the atmosphere were measured, with CO_2 flux values generally above 2 µmol m^{-2} s^{-1} (Fig. 4e). At the beginning of the measurement (Days 183 and 184), this classical scheme of CO_2 uptake at LT/Day and CO_2 degassing at LT/Night was perturbed and replaced by a strong CO_2 source to the atmosphere, also at LT/Day, reaching 12 µmol m^{-2} s^{-1} (Fig. 4e). During this event, PAR values were below 500 µmol m^{-2} s^{-1} at midday (Fig. 4a), and a particular mass of air coming from the south-southwest wind sector (180–225°) changed in speed, reaching 8 m s^{-1}, and in direction (Fig. 4c and d).

3.3 Autumn 2008 at Station 1

Contrary to the previous measurements, in September–October 2008 at Station 1, the Arcachon flat was a sink of CO_2 over the twenty days, with an average daily uptake of −0.2 ± 0.7 g C m^{-2} day^{-1} and values ranging from −1.2 to 1.2 g C m^{-2} day^{-1} (Table 1). Contrasting CO_2 flux variations were also observed with natural cycles from CO_2 flux values of −11 to 14 µmol m^{-2} s^{-1} (Fig. 5e). During this deployment, medium CO_2 sinks were measured at LT/Day, with values generally close to 5 µmol m^{-2} s^{-1} (i.e. Days 287 and 289), whereas weak CO_2 sources were found at LT/Night below 3 µmol m^{-2} s^{-1} (i.e. Days 286 and 288) (Fig. 5e). The PAR values were typical for the season, with some values close to 1250 µmol m^{-2} s^{-1} being measured at midday during sunny days. The PAR values were slightly higher than those measured during the same season in 2007 at Station 2, probably because of the presence of clouds during the four days of measurement. At Station 1, PAR values observed at midday decreased over the twenty days of measurement, from 1500 µmol m^{-2} s^{-1} to 1300 µmol m^{-2} s^{-1}, i.e. at a rate of -10 µmol m^{-2} s^{-1} each day (Fig. 5a). As noted in the previous measurements, reductions in CO_2 influxes at day and in CO_2 effluxes at night were observed with immersion. Indeed, during Day 276, the CO_2 flux shifted in less than one hour from −1.5 µmol m^{-2} s^{-1} at LT to −0.7 µmol m^{-2} s^{-1} with 30 cm of water, whereas the PAR remained high and constant (Fig. 5e). During flood tide on Night 279/280, CO_2 degassing decreased from 1.0 to 0.2 µmol m^{-2} s^{-1} in less than one hour after the tidal flat

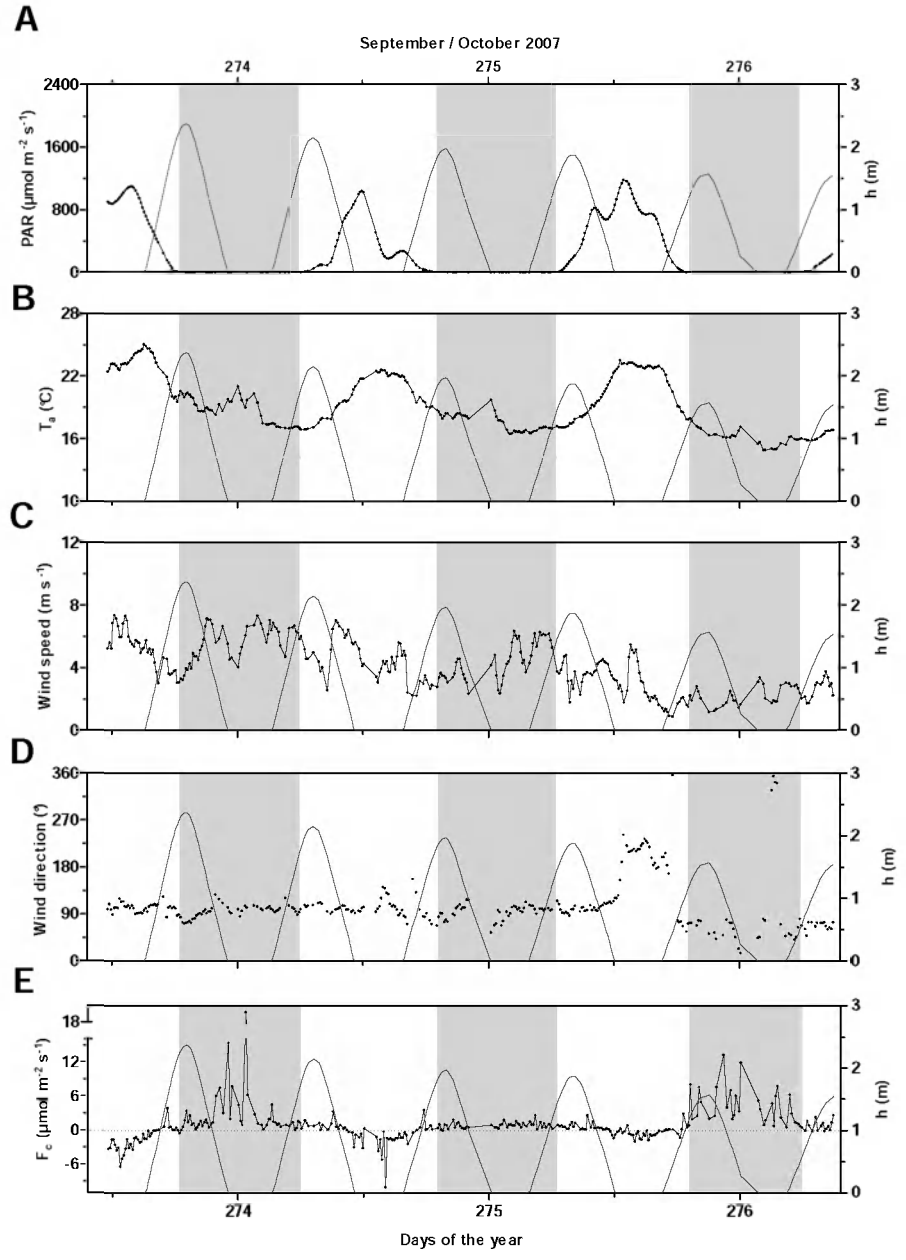

Fig. 3. Environmental parameters and carbon dioxide fluxes measured during the EC deployment in the Arcachon flat (St. 2) from 30 September at 11:35 to 3 October 2007 at 08:55 (GMT). **(A)** Photosynthetically active radiation ($\mu mol\,m^{-2}\,s^{-1}$) and water height (m); **(B)** temperature of the air (°C); **(C)** wind speed ($m\,s^{-1}$); **(D)** wind direction (°) and **(E)** carbon dioxide fluxes ($\mu mol\,m^{-2}\,s^{-1}$). Negative fluxes represent sinks of CO_2, and positive fluxes represent sources of CO_2 to the atmosphere by convention. Day 273 squares with 30 September 2007 and grey bands represent night periods. A PAR threshold of 20 $\mu mol\,m^{-2}\,s^{-1}$ was chosen to separate day and night cases, and low tide cases correspond to zero-water heights. A specific range for F_C **(E)** was chosen for a better visualisation of CO_2-flux variations.

immersion. Contrary to September–October 2007 at Station 2 and July 2008 at Station 1, CO_2 influxes were measured at HT/Night ($-0.3 \pm 1.3\,\mu mol\,m^{-2}\,s^{-1}$ on average, Table 1), as found during Night 282/283, with values reaching $-7\,\mu mol\,m^{-2}\,s^{-1}$ (Fig. 5e). In addition, a strong CO_2 emission of $14\,\mu mol\,m^{-2}\,s^{-1}$ was observed at LT/Day (Day 279) immediately after a sudden and concomitant increase in air temperature and wind speed (Fig. 5b and c) and a switch in wind direction to the 180–225° sector (Fig. 5d).

3.4 Spring 2009 at Station 1

In April 2009, the strongest CO_2 sink was measured in the Arcachon flat, with an average daily flux of

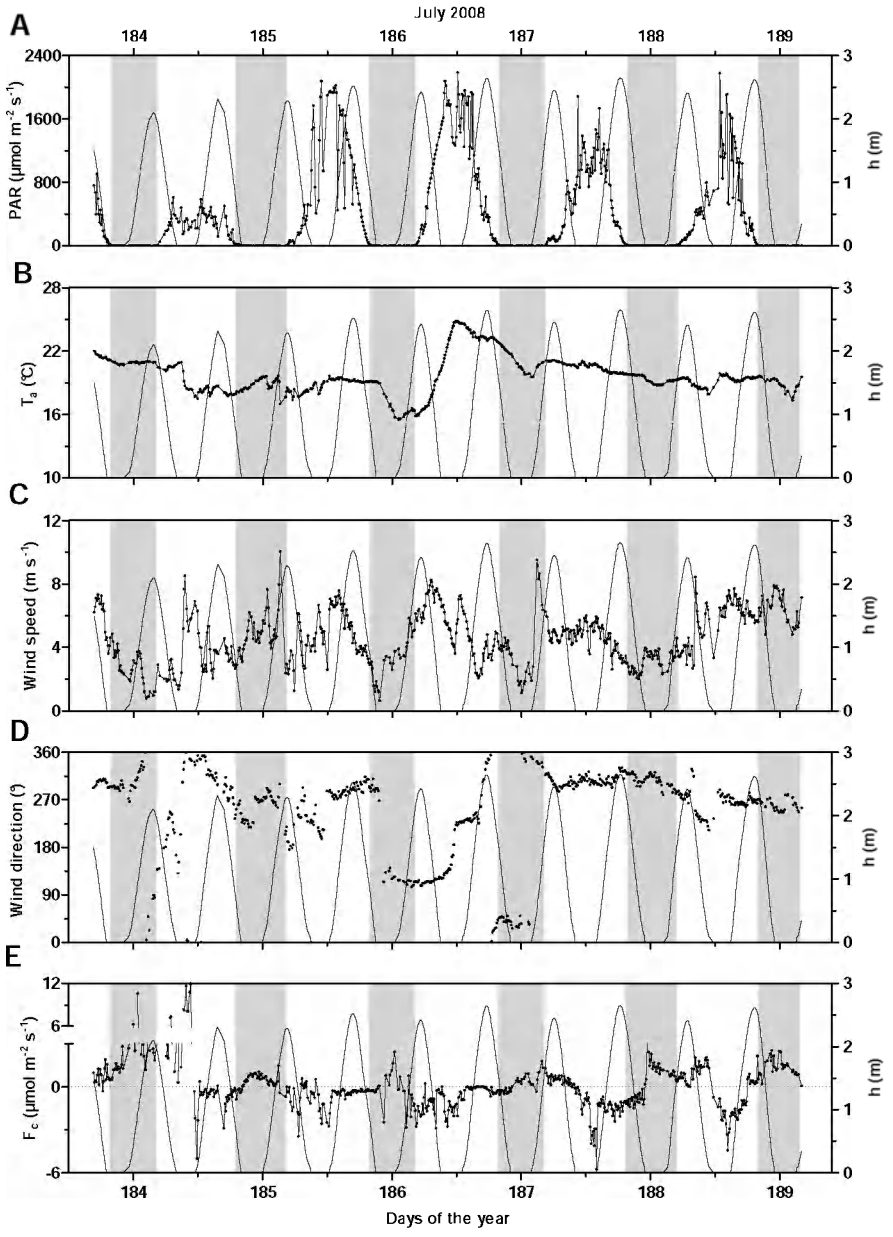

Fig. 4. Environmental parameters and carbon dioxide fluxes measured during the EC deployment in the Arcachon flat (St. 1) from 1 July at 16:40 to 7 July 2008 at 04:00 (GMT). **(A)** Photosynthetically active radiation PAR ($\mu mol\,m^{-2}\,s^{-1}$) and water height (m); **(B)** temperature of the air (°C); **(C)** wind speed ($m\,s^{-1}$); **(D)** wind direction (°) and **(E)** carbon dioxide fluxes ($\mu mol\,m^{-2}\,s^{-1}$). Negative fluxes represent sinks of CO_2, and positive fluxes represent sources of CO_2 to the atmosphere by convention. Day 183 squares with 1 July 2008 and grey bands represent night periods. A PAR threshold of $20\,\mu mol\,m^{-2}\,s^{-1}$ was chosen to separate day and night cases, and low tide cases correspond to zero-water heights. A specific range for F_c **(E)** was chosen for a better visualisation of CO_2 flux variations.

$-2.4 \pm 0.9\,g\,C\,m^{-2}\,day^{-1}$, the flat remaining a CO_2 sinks over each of the thirteen days of measurement (daily flux range: -4.3–$-0.9\,g\,C\,m^{-2}\,day^{-1}$, Table 1). No clear pattern was observed in contrast to the previous measurements, with CO_2 fluxes mostly always negative regardless of the diurnal or the tidal phase, ranging from -13 to $3\,\mu mol\,m^{-2}\,s^{-1}$, the largest sinks occurring at HT during the night 96–97 (Fig. 6e). However, large sinks of CO_2 also occurred at LT/Day (i.e. days 94, 95 and 103), and positive fluxes of CO_2 occurred in conditions of well-established LT at night (nights 92–93, 99–100, 100–101 and 101–102) (Fig. 6e). At LT/Day during Days 95 and 96, weaker CO_2 influxes corresponded to cold masses of air close to 13 °C with low wind speeds near $1\,m\,s^{-1}$ and wind directions from the south-southeast (135–

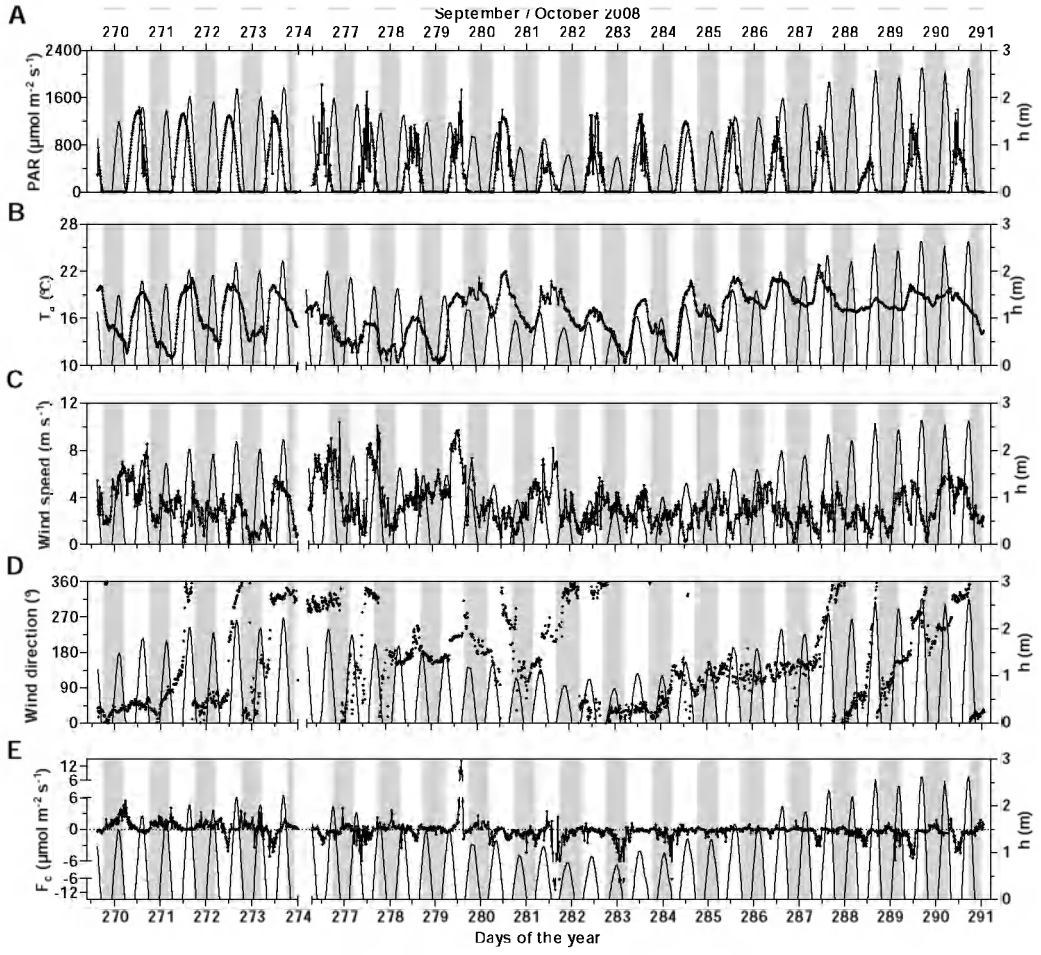

Fig. 5. Environmental parameters and carbon dioxide fluxes measured during the EC deployment in the Arcachon flat (St. 1) from 25 September at 15:10 to 17 October 2008 at 01:10 (GMT). **(A)** Photosynthetically active radiation PAR ($\mu mol\,m^{-2}\,s^{-1}$) and water height (m); **(B)** temperature of the air (°C); **(C)** wind speed ($m\,s^{-1}$); **(D)** wind direction (°) and **(E)** carbon dioxide fluxes ($\mu mol\,m^{-2}\,s^{-1}$). Negative fluxes represent sinks of CO_2, and positive fluxes represent sources of CO_2 to the atmosphere by convention. Day 269 squares with 25 September 2008, and grey bands represent night periods. Data between 30 September (00:10) and 2 October 2008 (07:10) could not be measured due to technical problems during the deployment. A PAR threshold of $20\,\mu mol\,m^{-2}\,s^{-1}$ was chosen to separate day and night cases, and low tide cases correspond to zero-water heights. A specific range for F_c **(E)** was chosen for a better visualisation of CO_2 flux variations.

180°) (Fig. 6b, c, d and e). In contrast to the three previous measurement periods, when LT/Night cases always corresponded to CO_2 releases to the atmosphere due to benthic respiration, in April 2009, CO_2 fluxes at LT/Night were either null or negative (Table 1 and Fig. 6e). In fact, these negative fluxes occurred during very short periods of LT/Night, at the end (Day 94) or at the beginning (Days 94/95 and 95/96) of the night and immediately after or before immersion (Fig. 6e). Negative F_c data corresponding to very short periods of LT/Night and very fast changes in CO_2 fluxes were potentially affected by flooded areas and then excluded from the averages (Table 1).

3.5 Wind direction and Zostera noltii cover

Figure 7 presents the occurrence of prevailing winds per sector for each period. Wind directions varied temporally according to the season and also spatially according to the station. In September–October 2007 at Station 2, the prevailing winds blew mostly from the east-southeast and east-northeast, with 60 % and 27 % of occurrence, respectively (Fig. 7a). In autumn 2008 at Station 1, no wind direction clearly prevailed; the north–northeast (0–45°) and south–southeast (135–180°) sectors both accounted for 20 % of the wind, and the 180–315° sector accounted for less than 10 % (Fig. 7b). During July 2008 and April 2009 at Station 1, wind direction also changed often, but consistent prevailing winds

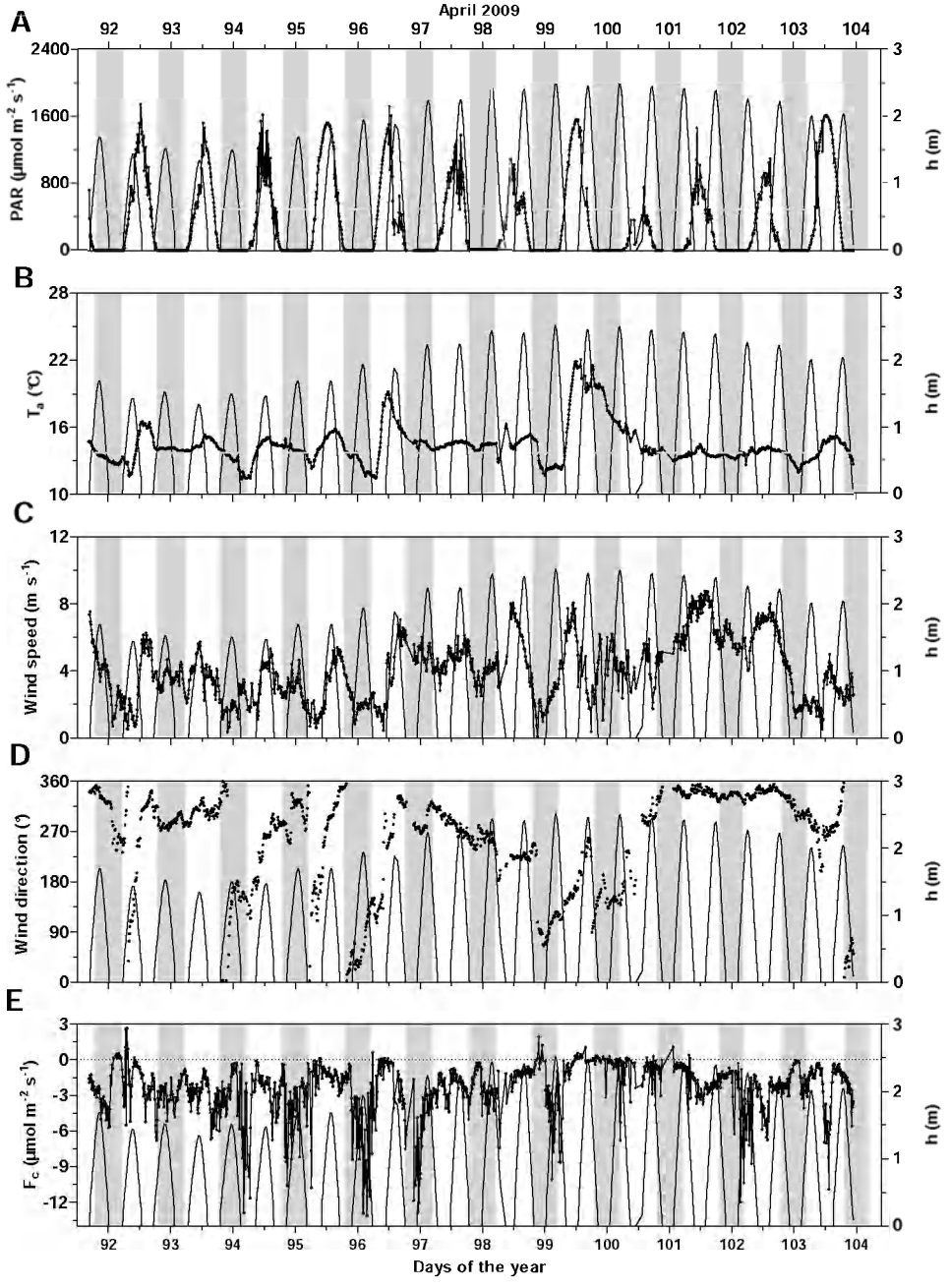

Fig. 6. Environmental parameters and carbon dioxide fluxes measured during the EC deployment in the Arcachon flat (St. 1) from 1 April at 16:30 to 13 April 2009 at 22:50 (GMT). **(A)** Photosynthetically active radiation PAR ($\mu mol\,m^{-2}\,s^{-1}$) and water height (m); **(B)** temperature of the air (°C); **(C)** wind speed ($m\,s^{-1}$); **(D)** wind direction (°) and **(E)** carbon dioxide fluxes ($\mu mol\,m^{-2}\,s^{-1}$). Negative fluxes represent sinks of CO_2, and positive fluxes represent sources of CO_2 to the atmosphere by convention. Day 91 squares with the 1 2009 and grey bands represent night periods. A PAR threshold of 20 $\mu mol\,m^{-2}\,s^{-1}$ was chosen to separate day and night cases, and low tide cases correspond to zero-water heights.

occurred from the 225–315° and the 270–360° sectors. Consequently, winds from the west–northwest were mostly observed during both seasons, reaching more than 40 % in summer 2008 and 30 % of occurrence in spring 2008 (Fig. 7c, d).

The analyses of satellite images of the tidal flat at LT/Day showed clear variations in the *Zostera noltii* seagrass cover according to wind directions for both stations (Table 2). In autumn 2007 at Station 2, seagrass cover was generally low (22 ± 14 % in average), ranging between 4 % and 51 % from

Table 2. NEP values (corresponding to mean LT/Day CO_2 fluxes ± standard deviation) and *Zostera noltii* covers derived from satellite image analyses from the Arcachon flat, at low tide during the day, according to sectors of wind direction (circle of 1000 m radius around the mast and split in 32 sectors of 11.25°). No satellite image matching with the deployment in July 2008 at Station 1 was available.

		NNE **0–45°**	ENE **45–90°**	ESE **90–135°**	SSE **135–180°**	SSW **180–225°**	WSW **225–270°**	WNW **270–315°**	NNW **315–360°**
Station 2 Autumn 2007	*Zostera noltii* cover (13/09/2007)	**19 %**	**25 %**	**27 %**	**17 %**	**4 %**	**14 %**	**15 %**	**51 %**
	NEP (µmol m^{-2} s^{-1})		**−0.9 ± 0.7**	**−2.1 ± 1.4**	**−2.1 ± 4.4**	**−0.7 ± 0.6**	**−0.7 ± 0.7**		
	Percentage of NEP data		4 %	61 %	7 %	21 %	7 %		
Station 1 Summer 2008	NEP (µmol m^{-2} s^{-1})			**−1.1 ± 0.9**	**−1.4 ± 0.3**	**−1.4 ± 0.6**	**−0.9 ± 0.9**	**−2.0 ± 1.4**	**−0.7 ± 0.2**
	Percentage of NEP data			11 %	6 %	14 %	18 %	47 %	4 %
Station 1 Autumn 2008	*Zostera noltii* cover (17/10/2008)	**98 %**	**93 %**	**86 %**	**70 %**	**95 %**	**99 %**	**99 %**	**98 %**
	Zostera noltii cover (08/09/2009)	**97 %**	**95 %**	**87 %**	**69 %**	**94 %**	**98 %**	**99 %**	**98 %**
	NEP (µmol m^{-2} s^{-1})	**−0.5 ± 1.5**	**−0.7 ± 1.3**	**−0.1 ± 0.9**	**−0.9 ± 1.0**	**−1.5 ± 2.6**	**−2.2 ± 2.0**	**−2.0 ± 1.1**	**−1.5 ± 1.2**
	Percentage of NEP data	9 %	17 %	14 %	21 %	9 %	6 %	12 %	12 %
Station 1 Spring 2009	*Zostera noltii* cover (24/06/2009)	**90 %**	**89 %**	**74 %**	**62 %**	**94 %**	**97 %**	**96 %**	**94 %**
	NEP (µmol m^{-2} s^{-1})			**−3.8 ± 3.6**	**−1.0 ± 1.6**	**−1.6 ± 1.0**	**−4.5 ± 2.6**	**−3.0 ± 1.5**	**−3.1 ± 1.2**
	Percentage of NEP data			6 %	19 %	8 %	7 %	32 %	28 %

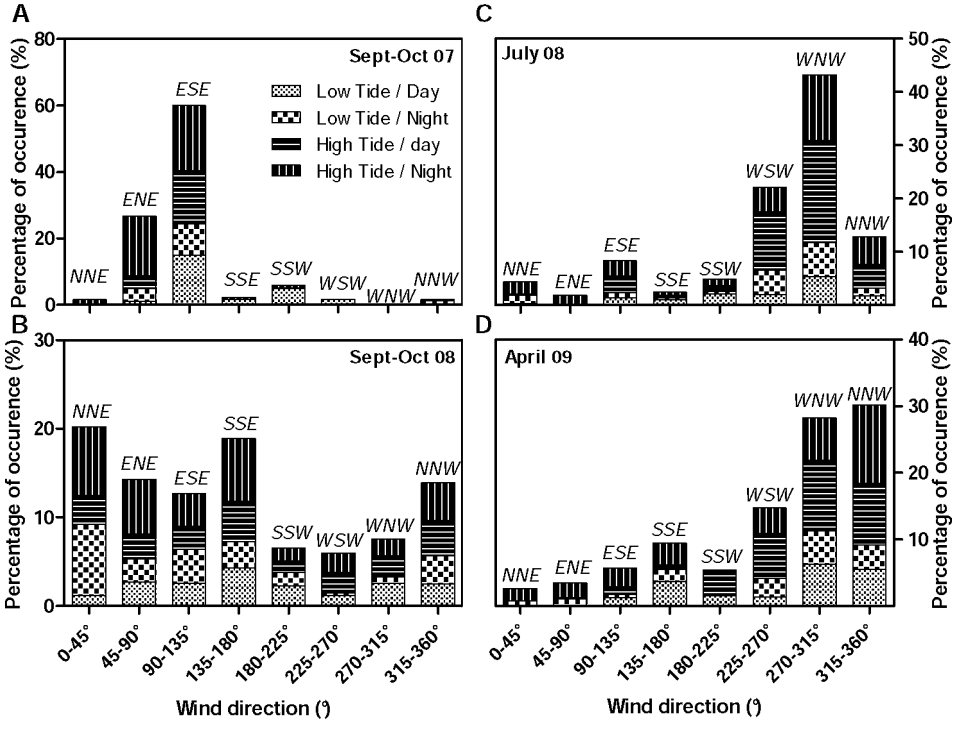

Fig. 7. The wind directions during the four EC measurements in the Arcachon flat by percentage of occurrence and functions to the tidal and diurnal rhythms (low tide/day, low tide/night, high tide/day and high tide/night). **(A)** 30 September to 3 October 2007 (St. 2), **(b)** 25 September to 17 October 2008 (St. 1), **(C)** 1 to 7 July 2008 (St. 1) and **(D)** 1 to 13 April 2009 (St. 1).

the south–southwest and east–southeast wind sectors, respectively (Table 2). A significant difference in the seagrass cover was computed between wind sectors 146.25–247.5°/78.5–146.25° with 4 ± 3 % (0–9 %) and 24 ± 13 % (7–37 %) respectively ($p = 0.0027$). In autumn 2008 at Station 1, higher *Zostera noltii* covers were measured than during the same season in 2007 at Station 2 (92 ± 10 % in average), with values ranging between 70 % (south-southeast) and 99 % (west-northwest) (Table 2). Similarly, a clear *Zostera noltii* seagrass cover variation was observed between wind sectors 11.25–168.75° and 168.75–360° with 86 ± 13 % (55–100 %) and 96 ± 5 % (80–100 %) respectively ($p = 0.0012$). The next year, in autumn 2009, exactly the same percentage of *Zostera noltii* cover was observed (92 ± 10 % in average),

between 69 and 99 % (Table 2). In regards to the spring deployment at Station 1 in 2009, no matching satellite image was available; the analysis of the image recorded on April 2010 (14/04), the year after the EC deployment, showed a very low seagrass cover, below 5 %, regardless of wind direction (data not shown). The image recorded on 24 June 2009, obtained ten weeks after this spring EC deployment, showed slightly lower seagrass cover than in late summer–autumn (87 ± 13 % in average, range: 62–97 %, Table 2) but higher than that measured previously, in early spring 2010. A variation in the seagrass cover was also observed between wind sectors 135–247.5° and 101.25–135°/247.5–360°, with 80 ± 22 % (36–99 %) and 91 ± 7 % (75–97 %) respectively ($p = 0.823$).

4 Discussion

4.1 Spatial and temporal variations of NEE in relation to NEP of the Arcachon flat

4.1.1 Diurnal and tidal changes in NEE at the different seasons

Throughout the diurnal and tidal cycles, variations in NEE were large, with the flat often rapidly shifting from source to sink. For instance, at Station 1 in July 2008 on Day 184 and daytime, NEE rapidly dropped from 12.0 µmol m^{-2} s^{-1} at low tide to -5.0 µmol m^{-2} s^{-1} as soon as the water submerged the flat. Inversely, at night, between Days 187 and 188, the CO_2 flux was -0.8 µmol m^{-2} s^{-1} at the end of the immersion and rose to 3.0 µmol m^{-2} s^{-1} at the beginning of the emersion (Fig. 4e). There are a number of processes that can induce these rapid changes in NEE, including benthic and planktonic GPP and CR, advection with water movements and air-water gas exchange. Although in the intertidal Wadden Sea, Zemmelink et al. (2009) found little dependency of CO_2 fluxes on the tide, this was not the case in the Arcachon flat. The effect of rising tide on CO_2 exchange was first reported by Houghton and Woodwell (1980) in a salt marsh. Kathilankal et al. (2008) reported a 46 % reduction in CO_2 uptake during emersion. In these salt marsh systems, part of the vegetation remains emerged even at high tide. In intertidal systems like Arcachon or the Wadden Sea, at low tide, benthic GPP and CR are theoretically the two main drivers of NEE. When the tide rises over the flat, benthic and planktonic communities contribute to GPP and CR, but their effect on NEE may not be immediate because water-air gas exchange is slow in comparison with the duration of the immersion. For instance, for typical conditions in coastal systems and a gas-transfer velocity of 10 cm h^{-1}, it takes 3.5 h for pCO_2 to decrease from 600 to 500 ppmv with gas exchange, which corresponds to a CO_2 flux of $\sim$1.2 µmol m^{-2} s^{-1}, comparable to what we observed here. Consequently, a negative water–air gradient can be created, for instance by phytoplankton at the mouth of the flat at low tide, then these CO_2-undersaturated waters can enter with the flood tide. This would generate a negative NEE in the flat at high tide, that would not result from the in situ NEP. Inversely, intense benthic and planktonic CR at high tide in the flat would not necessarily immediately generate an equivalent degassing of CO_2 to the atmosphere, with some of the CO_2 remaining in solution and being exported laterally with the subsequent ebb tide. Such CO_2 outwelling from intertidal systems to adjacent creeks and bays has been observed in many tidal wetlands (Cai et al., 2003; Wang and Cai, 2004; Borges et al., 2003).

The September 2007 measurements at Station 2 in the inner part of the flat provide a first and relatively simple scheme for conceptualising NEE dynamics in relation to NEP at the different phases of the day and the tide. During this experiment, we observed strong CO_2 uptake at LT/Day but CO_2 degassing during all other cases (Fig. 3e, Table 1). This suggests that at LT/Day, the tidal flat was autotrophic, whereas it was heterotrophic during the night and during immersion. In addition, CO_2 degassing at LT/Night and HT/Night was significantly higher ($p < 0.05$) than at HT/Day, which suggests that in the daytime during immersion, benthic and planktonic GPP significantly reduce CO_2 degassing from waters. Benthic GPP by microphytobenthos is controlled by light availability (Parsons et al., 1984) and is believed to be light limited during immersion. At Station 2, where the *Zostera noltii* cover was particularly low, microphytobenthos, could significantly be resuspended and contribute to planktonic GPP at the beginning of the flood tide (Guarini, 1998).

At Station 1, in the centre of the flat, patterns of CO_2 fluxes were fundamentally different, as uptake of atmospheric CO_2 were also observed during the immersion. This occurred during the day at the three periods of measurements and also during the night in September 2008 and in April 2009. In contrast, in July 2008, the flat was a source of CO_2 at HT/Night, being a sink at HT/Day (Table 1). Negative NEE during HT/Night demonstrates the impact of planktonic GPP at the outlet of the flat, followed by advection of CO_2-depleted water masses with the flood tide. Indeed, the channel and subtidal areas of the flat are the sites of development of phytoplankton blooms with high primary production rates, particularly in early spring (Glé et al., 2007, 2008). In April 2009, the uptake of atmospheric CO_2 during immersion at Station 1 was nearly two times higher at night time than at daytime (Table 1). This suggests that the CO_2 depletion of the waters may have occurred at daytime a few hours before, precisely when the water masses were at the mouth of the flat. On the contrary, the water present at daytime over the tidal flat absorbed less atmospheric CO_2, as it was present at the outlet of the flat around night time; this also suggests that during this spring period, GPP during immersion was lower in the flat than outside of the flat, consistent with results of Glé et al. (2007) who showed planktonic primary production always higher in external waters.

In July and September 2008, NEE during immersion at Station 1 showed different patterns. In September, NEE was slightly negative ($\sim -0.2\,\mu mol\,m^{-2}\,s^{-1}$; Table 1) at both HT/Day and HT/Night, suggesting, as in April 2009, a predominant role of advection of CO_2-depleted waters from the mouth of the flat. In contrast, in July 2008, the water in the flat was a sink of CO_2 at daytime but a source of CO_2 at night (Table 1), meaning that advection phenomena were probably less important than metabolic processes inside the flat itself, by both planktonic and benthic communities. CO_2 uptake at LT/Day measured by EC was systematically reduced at HT/Day during the four deployments (Figs. 3, 4, 5, 6e and Table 1). This was especially true in the summer and autumn seasons in 2008 at Station 1, when the *Zostera noltii* cover was maximal. This could be due to lower photosynthetic activity of primary producers due to light limitation in the presence of water, or to a delay in water-air gas equilibration, as previously discussed. Little is known about seagrass metabolism in coastal flats, especially on NPP and photosynthetic efficiency during air-exposed versus immersed conditions (Silva et al., 2005, 2008; Abril, 2009; Silva and Santos, 2009; Clavier et al., 2011). Using benthic chambers, Clavier et al. (2011) observed in the Banc d'Arguin (Mauritania) carbon fluxes by *Zostera noltii* beds greater under water than when exposed to air. Another key factor for CO_2 uptake by air-exposed *Zostera noltii* is the leaf water content (Leuschner et al., 1998). In tidal flats, the existence of depressions in the sediment at low tide can retain enough amount of water to maintain leaf hydration, and allow high photosynthetic rates of the seagrass and rapid air-water CO_2 diffusion (Silva et al., 2005). Because CO_2 diffuses much slowly through the water-air interface than through air, the carbon uptake we observed during tidal flooding in the flat is probably more related to the initial pCO_2 of waters entering the flat, than to the in situ photosynthetic activity of *Zostera noltii* underwater.

Finally, another type of physical processes was driving CO_2 fluxes in the flat, and resulted in very strong CO_2 degassing to the atmosphere at LT/Day at Station 1, in July 2008 on Day 184 (Fig. 4e), and in September–October 2008 on Day 279 (Fig. 5e). Such singular CO_2 degassing was too high and rapid to be explained by biological respiration, and was obviously caused by destocking processes linked to the onset of atmospheric turbulence (high wind speeds). These destocking events were not related to the tide; they occurred during the emersion in the morning and were concomitant with sudden changes in wind direction.

4.1.2 Relationship between low tide CO_2 fluxes and the distribution of *Zostera noltii* meadows

CO_2 fluxes between the Arcachon flat at low tide and the atmosphere showed important spatial and temporal variations. Significant spatial and temporal differences in *Zostera noltii* cover were also observed from satellite images (Table 2). For the low tide conditions, we can assume that benthic CR was equivalent to NEE at night (Rocha and Goulden, 2008), and benthic NEP was equivalent to NEE averaged over the daytime. GPP at low tide can be calculated as the NEE at night minus the NEE during the day, as presented in Table 3. In autumn 2007 at Station 2 with a low *Zostera noltii* density, a particularly high GPP of $4.4 \pm 4.1\,\mu mol\,m^{-2}\,s^{-1}$ was calculated, the CR showing the highest value, with $2.7 \pm 3.7\,\mu mol\,m^{-2}\,s^{-1}$ (Table 3). In contrast, in autumn 2008 at Station 1 with a high *Zostera noltii* density, a slightly low GPP of $1.1 \pm 2.0\,\mu mol\,m^{-2}\,s^{-1}$ was found, the CR being only $0.2 \pm 1.1\,\mu mol\,m^{-2}\,s^{-1}$ (Table 3). At both stations, rapid changes in CO_2 fluxes (NEP) were observed in relation to wind direction and seagrass cover; the most negative (highest NEP) and the less negative (lowest NEP) CO_2 fluxes matched the highest and the lowest seagrass cover, respectively (Table 2). For instance, in September 2007 at Station 2, mean fluxes from the 78.75–90° wind sector with a seagrass cover of $24 \pm 13\,\%$ were -2.2 ± 1.8 whereas those from the 146.25–247.5° sector with a $4 \pm 3\,\%$ cover were $-0.6 \pm 0.6\,\mu mol\,m^{-2}\,s^{-1}$. Such correspondence between NEP at low tide and seagrass cover was observed at all stations and seasons (Table 2). These results indicate that *Zostera noltii* greatly contribute to the NEP in the central part of the flat, from spring to autumn. In areas where the *Zostera noltii* cover remains low all year round like the inner part of the flat (Plus et al., 2010), microphytobenthos communities potentially play a large role in the benthic metabolism and CO_2 fluxes at low tide. Indeed, at Station 2, the average computed NEP was slightly higher than at Station 1, but CR and thus the GPP were much higher than at Station 1 (Table 3). Such high GPP by microphytobenthos at low tide has been reported in many temperate intertidal mudflats (Guarini, 1998; Spilmont et al., 2006). These high GPP values are associated with high CR values at night due to heterotrophic bacteria (Hubas et al., 2006) and consistent with our observation with the EC at Station 2 (Table 3). In particular, Goto et al. (2001) have shown that benthic bacteria can utilize exudates from microphytobenthos. Also, high CR rates can be accounted for by the intense grazing of meiofauna and macrofauna on microphytobenthos, the latter being easily and rapidly transferred toward superior benthic heterotrophic components (Middelburg et al., 2000; Spilmont et al., 2006). Our EC data also reveal a clear seasonal cycle at Station 1, with a decrease of NEP from April through July to September (Table 3), a temporal pattern very consistent with the growing cycle of *Zostera noltii* (Auby and Labourg, 1996). There were probably also some changes in the contribution of the benthic primary producers (*Zostera noltii*, associated epiphytes and benthic microalgae) over the course of the year, that could occur in a relatively constant rate of production at the community scale, as shown by Ouisse et al. (2010) using static chambers.

GPP and CR calculations could not be performed from the EC data obtained in April 2009 (Station 1); CO_2 fluxes

Table 3. Comparison of NEP components at low tide for the autumn season at the two stations and in summer at Station 1. NEP was assumed as NEE at low tide during daytime, CR was assumed as NEE at low tide during the night, and GPP was assumed as the sum of NEP and CR. Notice that F_c values obtained in July 2008 during the beginning of the experiment (Days 183, 184) and in September–October 2008 (Day 279) have been discarded for calculations, representing destocking but not biological degassing by respiration (Figs. 5f and 6f). The GPP and CR calculations for the spring 2009 period at Station 1 were not possible because of the slight negative averaged flux value obtained at Low Tide/Night (see discussion). *Zostera noltii* covers for the April 2009 flux data are derived from a SPOT image from ten weeks later (26 June 2009) and are thus probably much higher than during the flux measurements.

	Zostera noltii cover (%)	NEP ($\mu mol\ m^{-2}\ s^{-1}$)	CR ($\mu mol\ m^{-2}\ s^{-1}$)	GPP ($\mu mol\ m^{-2}\ s^{-1}$)
September/October 2007 (Station 2)	22 ± 14	1.7 ± 1.7	2.7 ± 3.7	4.4 ± 4.1
July 2008 (Station 1)		1.5 ± 1.2	1.0 ± 0.9	2.5 ± 1.5
September/October 2008 (Station 1)	92 ± 10	0.9 ± 1.7	0.2 ± 1.1	1.1 ± 2.0
April 2009 (Station 1)	87 ± 13	2.7 ± 2.0		

over the mudflat were null or slightly negative at LT/Night and could not be attributed to benthic CR. In the unvegetated tidal flat of the Wadden Sea at the same season, Zemmelink et al. (2009) reported null and negative CO_2 fluxes with both EC and chamber techniques. Several processes could partly explain these fluxes in the Arcachon mudflat during this season, when the *Zostera noltii* density was low and microphytobenthic also contributed to NEP. First, microphytobenthic cells can migrate down to deeper layers of the sediment at night as protection against grazing by deposit-feeders (Blanchard et al., 2001); thus, respiration would not release CO_2 to the atmosphere but deeper into the sediments. Second, CO_2 generated by benthic respiration could be almost entirely involved in the dissolution of carbonate shells and not released to the atmosphere, as occurred for instance in a Mediterranean seagrass meadow (*Posidonia oceanica*) in winter (Barrón et al., 2006). The Arcachon flat represents an important stock of carbonates of about 120 Mt of several shellfish species as *Crassostrea gigas* contributing to 95 % (D. M. X. De Montaudouin, personal communication, 2011). From the end of the reproduction season (November) to the spat removing in spring, juvenile bivalves are particularly sensitive to dissolution-induced mortalities as shown by Green et al. (2004) in laboratory on the juvenile bivalve *Mercenaria mercenaria*. Thus, $CaCO_3$ dissolution could occur in wet mud sediments in presence of such shellfishes patchy distributed on the tidal flat.

To complete our analysis on the controlling factors of CO_2 fluxes at LT/Day, NEE-PAR relations ranked by wind direction and *Zostera noltii* cover were analysed (Table 4). Significant ($p < 0.01$) negative or positive correlations were obtained at Station 1 (Table 4). Negative correlations occurred in areas with a high *Zostera noltii* cover (>93 %), whereas positive correlations occurred in areas with lower *Zostera noltii* cover (<83 %). Note that for the April 2009 period, the *Zostera noltii* cover was obtained from a SPOT image from 24 June 2009, so the real cover during the measurements is probably much lower. Nevertheless, the first two sectors in Table 4 for this season have much higher seagrass covers than the last two sectors. As *Zostera noltii* growths in well-defined areas from spring to summer (Plus et al., 2010), differences in NEE-PAR correlations are indeed related to large differences in the seagrass cover in spring, during the measurements. These negative correlations between NEE and PAR (or positive correlations between NEP and the intensity of available light) reveal an optimal adaptation of the plants to the environmental conditions created by the solar radiation, such as temperature, humidity and light. Similar negative correlations have been observed with EC by Morison et al. (2000) for the C_4 aquatic grass *Echinochloa polystachya* of the Amazon and by Kathilankal et al. (2008) for the *Spartina alterniflora* in a salt marsh on the eastern coast of Virginia. Using static chambers, Silva et al. (2005) obtained the same results for *Zostera noltii* meadows in the intertidal flats of the Ria Formosa flat in Portugal. The fact that these negative correlations occur in areas with the highest *Zostera noltii* cover confirms that the seagrass in the Arcachon flat grows in optimal light condition and that its photosynthetic activity dominates the CO_2 uptake at low tide where the plant prevails. To the contrary, the three significant positive linear regressions observed in areas with lower *Zostera noltii* cover (Table 4) suggests another dominant metabolism that responses differently to the light intensity. In intertidal mudflats dominated by microphytobenthos, negative correlations between CO_2 fluxes and irradiance have been systematically observed with static chambers (Guarini, 1998; Spilmont et al., 2006; Migné et al., 2007). There was no significant correlation between NEE and air temperature during these three measurements periods, which precludes the hypothesis of a stimulation of CR by surface heating. Photoinhibition of photosynthesis by microphytobenthos may occur, but this mechanism has been observed

Table 4. F_c – PAR relationships obtained at low tide during the day in the Arcachon flat according to wind directions; F_c: EC Carbon dioxide fluxes; PAR: photosynthetically active radiation; R^2: coefficient of determination; p: probability that the slope is significantly non-zero; N: number of values used for each regressions. F_c values obtained in July 2008 during the beginning of the experiment (days 183, 184) and in September–October 2008 (day 279) have been discarded representing destocking but not biological degassing by respiration (Figs. 5f and 6f). Only significant linear regressions (p value < 0.01) are presented. Equations in bold and in italic represent negative and positive F_c – PAR relationships respectively. *Zostera noltii* covers for the April 2009 flux data are derived from a SPOT image from ten weeks later (26 June 2009) and are thus probably much higher than during the flux measurements.

	Zostera noltii cover (%)	Wind Sector (°)	Fit F_c – PAR linear regression	PAR range (µmol m^{-2} s^{-1})	R^2	p	N
July 2008 (Station 1)		191.5–270 + 315–326.25	**$[-0.00084 \pm 0.00025]\ x + [0.115 \pm 0.369]$**	[410–2185]	0.31	0.0031	26
September/ October 2008 (Station 1)	98 ± 0.5 (98 ~ 99)	225–270	**$[-0.0042 \pm 0.00085]\ x + [0.385 \pm 0.592]$**	[153–1154]	0.48	< 0.0001	28
	83	45–56.25	*$[0.00155 \pm 0.00042]\ x - [1.07 \pm 0.37]$*	[177–1333]	0.34	0.0012	28
April 2009 (Station 1)	93 ± 2 (91 ~ 95)	315–360	**$[-0.0024 \pm 0.00045]\ x - [1.51 \pm 0.327]$**	[40–1468]	0.25	< 0.0001	84
	96 ± 3 (93 ~ 98)	225–270	**$[-0.0071 \pm 0.00157]\ x + [5.398 \pm 2.223]$**	[904–1614]	0.52	0.0002	21
	79 ± 4 (75 ~ 82)	101.25–135	*$[0.0084 \pm 0.0014]\ x - [7.735 \pm 0.816]$*	[35–1159]	0.66	< 0.0001	20
	76 ± 23 (36 ~ 99)	135–225	*$[0.00155 \pm 0.000264]\ x - [2.526 \pm 0.271]$*	[26–1567]	0.30	< 0.0001	83

primarily in laboratory and rarely in field conditions (Blanchard and Cariou-Le Gall, 1994). Alternatively, it has been shown that microphytobenthic cells can migrate vertically through the sediments to protect them in response to long periods of light exposure at LT/Day as behavioural process of photo-acclimatisation (Blanchard et al., 2004; Serôdio et al., 2008). More investigation is needed to elucidate these positive NEE-PAR correlations associated to lower seagrass covers obtained in September–October 2008 and April 2009.

4.2 Implication for the carbon cycle in the Arcachon flat and the coastal ocean

Table 5 summarizes benthic and pelagic metabolic fluxes at low and high tides estimated so far in the Arcachon flat with different methods. NPP, GPP and CR of *Zostera noltii* meadows as derived from biomass, static chamber incubations and EC measurements were relatively consistent. The slightly higher average value of NPP obtained here with the EC technique might be explained by a contribution of lower winter values to the yearly average measured with chambers, as our EC data do not contain winter measurements. Also, low NCP values were recorded in May 2006 by chambers (near 0.2 g C m^{-2} d^{-1}) when *Zostera noltii* meadows are usually already well developed at this season (Auby, 1991), which suggests that the site for static chamber deployment was not fully representative. With regards to the microphytobenthic community, contrasted GPP values from 0.09 (Auby, 1991) to 4.55 (this study) g C m^{-2} day^{-1} have been obtained using biomass and EC measurements respectively. Benthic production estimations from biomass measurements remain approximate because they do not account for re-suspension of the surface sediments (Guarini, 1998). Similarly, contrasted CR values between 0.27 and 2.83 g C m^{-2} day^{-1} have been obtained using benthic chamber and EC respectively. These results attest for the heterogeneity encountered between methodologies in particular in unvegetated sediments. The results obtained by EC presented in this study suggest the occurrence of two superimposed metabolic carbon cycles in the Arcachon flat, functioning at different timescales: a rapid (tide or days) C cycling (high GPP and CR), ensured by microphytobenthic communities at Station 2, and a slow (seasonal) C cycle (low GPP and CR), ensured by the seagrass meadows at Station 1. However, such statement should be confirmed after a more precise method validation as it is in contradiction with the conclusions of Ouisse et al. (2010) in the bay of Morlaix (France), where static chambers gave higher metabolic fluxes in seagrass meadows than in microphytobenthic communities. Concerning metabolic fluxes during the immersion, our EC measurements from spring to autumn at the central part of the flat gives a total pelagic and benthic NEP very close to the annual average of phytoplanktonic NPP values obtained by Glé et al. (2008) with ^{14}C incubations. It suggests that benthic NPP of the *Zostera noltii* meadows that potentially contributes to the NEP obtained by the EC method could compensate planktonic respiration, which was not documented in the Arcachon flat. Indeed, in *Zostera noltii* meadows of the Banc d'Arguin (Mauritania), Clavier et al. (2011) reported larger GPP in benthic chamber during the immersion than in static chambers during the emersion. Finally, as discussed previously, CO_2 fluxes at high tide as measured with the EC measurements are not totally related to the instantaneous metabolism in the sediment and the water, and are affected by some delays in water-air equilibration.

The large discrepancy between numbers in Table 5, due to methodological difficulties, spatial and temporal heterogeneity and the extremely dynamic character of tidal flat ecosystems, precludes at the moment a precise carbon budget of the flat. In addition, net CO_2 exchange between the flat and the atmosphere cannot be extrapolated on an annual basis, as EC winter data are lacking. Nevertheless these data reveal a very

Table 5. Benthic and pelagic metabolic flux estimations in the Arcachon tidal flat (in $g\,C\,m^{-2}\,day^{-1}$) – flux comparisons obtained by Eddy Covariance (this study); short incubations, i.e. benthic chambers (at three different seasons and over muddy and seagrass stations, D. D. Davoult et al., personal communication, 2008), ^{14}C measurements at incident light (year 2003, Glé et al., 2008); and biomass and Chlorophylle-*a* measurements (Auby, 1991; A. I. Auby, personal communication, 2011). NCP: net community production; NPP: net primary production; GPP: gross primary production and CR: community respiration.

$g\,C\,m^{-2}\,day^{-1}$	Primary producers	NCP	NPP	GPP	CR	Methods	References
Low Tide – Benthic Metabolism	*Zostera noltii*		0.2–1.5			Biomasses (Dry Weight)	A. I. Auby (pers. comm., 2011)
		0.5		1.22	0.72	Benthic chambers CO_2 fluxes	D. D. Davoult et al. (pers. comm., 2008) from 2005 to 2007 (in Mar, May and Sep)
		1.25		1.86	0.61	Eddy Covariance CO_2 fluxes	this study (Station 1, LT in Jul and Sep 2008)
	Microphytobenthos			0.09–0.22		Chlorophylle-*a* concentrations	Auby (1991)
				0.29–0.32			A. I. Auby (pers. comm., 2011)
		1.31		1.58	0.27	Benthic chambers CO_2 fluxes	D. D. Davoult et al. (pers. comm., 2008) from 2005 to 2007 (in Mar, May and Sep)
		1.72		4.55	2.83	Eddy Covariance CO_2 fluxes	this study (Station 2, in Sep–Oct 2007)
High Tide – Benthic & Pelagic Metabolism	Phytoplankton All		0.25			^{14}C short incubations at incident light	Glé et al. (2008) (year 2003)
		0.21		0.98	0.78	Eddy Covariance CO_2 fluxes	this study (Station 1, HT in Jul 2008)

active C cycling in the flat, autotrophic and heterotrophic activities being of the same order of magnitude and CO_2 being fixed preferentially at LT and daytime, being to a large extend released again to the atmosphere at other periods. This is very different from other coastal systems like for instance estuaries, which are generally net heterotrophic and CO_2 emitters all year round (Gattuso et al., 1998; Borges, 2005). In spring, the Arcachon flat represented a net sink of CO_2 of $-2.4\,g\,C\,m^{-2}\,day^{-1}$, whereas in summer and early autumn, it acted either as a small source or sink of CO_2, with 0.1 and -0.2–$0.5\,g\,C\,m^{-2}\,day^{-1}$, respectively. Such carbon fluxes are similar to or greater than those computed in the other tidal flats in France and in the Netherlands within a range of -1.9–$0.2\,g\,C\,m^{-2}\,day^{-1}$ (Migné et al., 2004; Spilmont et al., 2006; Zemmelink et al., 2009). They remained low compared to other tidal systems, such as salt or freshwater marshes with flux values from -0.8 to $0.4\,g\,C\,m^{-2}\,day^{-1}$ (Houghton and Woodwell, 1980; Rocha and Goulden, 2008) or as European estuaries that degas large quantities of CO_2 to the atmosphere from 1.2 to $9.1\,g\,C\,m^{-2}\,day^{-1}$ in average (Frankignoulle et al., 1998). One major property of intertidal ecosystems is their capacity to fix atmospheric carbon and export it to the adjacent marine areas with the water (Yan et al., 2008; Guo et al., 2009). Indeed, in such environments, lateral fluxes, i.e. advection, induced by the tide rhythm are significant components of the carbon budget. For instance, Guo et al. (2009) showed that estuarine vegetated wetlands, though acting as a carbon sinks, could export organic matter with tides to nearby estuarine and coastal waters, which fuel carbon emission from the receiving ecosystems. This was also concluded by Cai (2011) and Wang and Cai (2004) who qualified these receiving waters as "apparent heterotrophic", supported by CO_2 and organic carbon advection from tidal wetlands. Consequently, to go further on the carbon budget of the Arcachon flat, additional measurements of water pCO_2 during tidal cycles at the mouth, combined with more intensive EC CO_2 fluxes would be necessary.

Acknowledgements. This study was supported by the ANR project PROTIDAL coordinated by Pierre Anschutz and also by the Aquitaine region that has financed the EC system. We thank all the referees for their constructive comments that improved the clarity and overall quality of the manuscript. We are grateful to Guillaume Detandt, Georges Oggian, Dominique Serça for their help for the EC deployment and D. Davoult for providing unpublished static chamber data. This work was supported by the Centre National d'Etudes Spatiales (CNES, TOSCA SYNIHAL). It is based on observations with High Resolution Visible instruments embarked on SPOT satellites. We acknowledge the Kalideos teams for giving us access the satellite image database.

Edited by: E. Marañón

The publication of this article is financed by CNRS-INSU.

References

Abril, G.: Comment on: "Underwater measurements of carbon dioxide evolution in marine plant communities: A new method" by J. Silva et al. Estuarine, Coast. Shelf Sci., 82, 357—360, 2009.

Abril, G., Etcheber, H., Delille, B., Frankignoulle, M., and Borges, A. V.: Carbonate dissolution in the turbid and eutrophic Loire estuary, Mar. Ecol. Prog. Ser., 259, 129–138, 2003.

Amanieu, M.: Recherches écologiques sur la faune des plages abritées et des étangs saumâtres de la région d'Arcachon, PhD Thesis, Université Bordeaux 1, 234 pp., 1967.

Aubinet, M., Grelle, A., Ibrom, A., Rannik, U., Moncrieff, J., Foken, T., Kowalski, A. S., Martin, P. H., Berbigier, P., Bernhofer, C. H., Clement, R., Elbers, J., Granier, A., Grunwald, T., Morgenstern, K., Pilegaard, K., Rebmann, C., Snijders, W., Valentini, R., and Vesala, T.: Estimates of the annual net carbon and water exchange of European forests: the EUROFLUX methodology, Adv. Ecol. Res., 30, 113–175, 2000.

Auby, I.: Contribution à l'étude des herbiers de *Zostera noltii* dans le bassin d'Arcachon, PhD thesis, Université Bordeaux 1, 234 pp., 1991.

Auby, I. and Labourg, P. J.: Seasonal dynamics of *Zostera noltii* Hornem. in Bay of Arcachon (France), J. Sea Res., 35, 269–277, 1996.

Baldocchi, D. D.: Assessing the eddy covariance technique for evaluating carbon dioxide exchange rates of ecosystems: past, present and future, Glob. Change Biol., 9, 479–492, 2003.

Baldocchi, D. D., Hincks, B. B., and Meyers, T. P.: Measuring biosphere-atmosphere exchanges of biologically related gases with micrometeorological methods, Ecology, 5, 1331–1340, 1988.

Barillé, L., Robin, M., Harin, N., Bargain, A.. and Launeau, P.: Increase in seagrass distribution at Bourgneuf Bay (France) detected by spatial remote sensing, Aquatic Botany, 92, 185–194, 2010.

Barrón, C., Duarte, C. M., Frankignoulle, M., and Borges A. V.,Organic carbon metabolism and carbonate dynamics in a Mediterranean seagrass (*Posidonia oceanica*) meadow, Estuaries and Coasts, 29, 417–426, 2006.

Blanchard, G. F. and Cariou-Le Gall, V.: Photosynthetic characteristics of microphytobenthos in Marennes-Oléron Bay, France: preliminary results, J. Exp. Mar. Biol. Ecol., 182, 1–14, 1994.

Blanchard, G. F., Guarini, J. M., Orvain, F., and Sauriau, P. G.: Dynamic behaviour of benthic microalgal biomass in intertidal mudflats, J. Exp. Mar. Biol. Ecol., 264, 85–100, 2001.

Blanchard, G. F., Guarini, J. M., Dang, C., and Richard, P.: Characterizing and quantify photoinhibition in intertidal microphytobenthos, J. Phycol., 40, 692–696, 2004.

Borges, A. V.: Do we have enough pieces of the jigsaw to integrate CO_2 fluxes in the coastal ocean?, Estuaries, 28, 3–27, 2005.

Borges, A. V., Djenidi, S., Lacroix, G., Théate, J., Delille, B., and Frankignoulle, M.: Atmospheric CO_2 flux from mangrove surrounding waters, Geophys. Res. Lett., 30, 1558, doi:10.1029/2003GL017143, 2003.

Borges, A. V., Delille, B., and Frankignoulle, M.: Budgeting sinks and sources of CO_2 in the coastal ocean: diversity of ecosystems counts, Geophys. Res. Lett., 32, LI4601, doi:10.1029/2005GL023053, 2005.

Borges, A. V., Schiettecatte, L.-S., Abril, G., Delille, B., and Gazeau, F.: Carbon dioxide in European coastal waters, Estuarine, Coast. Shelf Sci., 70, 375–387, 2006.

Burba, G. and Anderson, D.: Introduction to the Eddy Covariance method: General Guidelines and Conventional Workflow, Licor, Inc., 1–141, 2005.

Cai, W.-J.: Estuarine and Coastal Ocean Carbon Paradox: CO_2 Sinks or Sites of Terrestrial Carbon Incineration?, Annu. Rev. Mar. Sci., 3, 123–145, doi:10.1146/annurev-marine-120709-142723, 2011.

Cai W.-J. and Wang, Y.: The chemistry, fluxes and sources of carbon dioxide in the estuarine waters of the Satilla and Altamaha Rivers, Georgia, Limnol. Oceanogr., 43, 657–668, 1998.

Cai, W.-J., Wang, Z., and Wang, Y.: The role of marsh-dominated heterotrophic continental margins in transport of CO_2 between the atmosphere, the land-sea interface and the ocean, Geophys. Res. Lett., 30, 1849, doi:10.1029/2003GL017633, 2003.

Chapin, F. S., Woodwell, G. M., Randerson, J. T., Rastetter, E. B., Lovett, G. M., Baldocchi, D. D., Clark, A., Harmon, M. E., Schimel, D. S., Valentini, R., Wirth, C., Aber, J. D., Cole, J. J., Goulden, M. L., Harden, J. W., Heimann, M., Howarth, R. W., Matson, P. A., McGuire, A. D., Melillo, J. M., Mooney, H. A., Neff, J. C., Houghton, R. A., Pace, M. L., Ryan, M. G., Running, S. W., Sala, O. E., Schlesinger, W. H., and Schulze, E. D.: Reconciling Carbon-cycle Concepts, Terminology, and Methods, Ecosystems, 9, 1041–1050, 2006.

Chauvaud, L., Thompson, J. K., Cloern, J. E., and Thouzeau, G.: Clams as CO_2 generators: The *Potamocorbula amurensis* example in San Francisco Bay, Limnol. Oceanogr., 48, 2086–2092, 2003.

Clavier, J., Chauvaud, L., Carlier, A., Amice, E., Van der Geest, M., Labrosse, P., Diagne, A., and Hily, C.: Aerial and underwater carbon metabolism of a *Zostera noltii* seagrass bed in the Banc d'Arguin, Mauritania, Aquatic Botany, 95, 24–30, 2011.

Duarte, C. M., Marbà, N., Gacia, E., Fourqurean, J. W., Beggins, J., Barrón, C., and Apostolaki, E. T.: Seagrass community metabolism: assessing the carbon sink capacity of seagrass meadows, Global Biogeochem. Cy., 24, 1–8, 2010.

Foken, T.: Angewandte Meteorologie, Mikrometeorologische Methoden, Springer, Heidelberg, 289 pp., 2003.

Foken, T. and Wichura, B.: Tools for quality assessment of surface-based flux measurements, Agr. Forest Meteorol., 78, 83–105, 1996.

Foken, T., Skeib, G., and Richter, S. H.: Dependence of the integral turbulence characteristics on the stability of stratification and their use for Doppler-Sodar measurements, Z. Meteorol., 41, 311–315, 1991.

Foken, T., Jegede, O. O., Weisensee, U., Richter, S. H., Handorf, D., Görsdorf, U., Vogel, G., Schubert, U., Kirzel, H.-J., and Thier-

mann, V.: Results of the LINEX-96/2 Experiment., Deutscher Wetterdienst, Forschung und Entwicklung, Arbeitsergebnisse, 48, 75 pp., 1997.

Frankignoulle, M., Abril, G., Borges A.V., Bourge, I., Canon, C., Delille, B., Libert, E., and Théate, J. M.: Carbon dioxide emission from European estuaries, Science, 282, 434–436, 1998.

Gattuso, J.-P., Frankignoulle, M., and Wollast, R.: Carbon and carbonate metabolism in coastal aquatic systems, Annual Review Ecology Systematics, 29, 405–433, 1998.

Gazeau, F., Smith, V. S., Gentili, B., Frankignulle, M., and Gattuso, J. P.: The European coastal zone: characterization and first assessment of ecosystem metabolism, Estuarine, Coast. Shelf Sci., 60, 673–694, 2004.

Glé, C., Amo, Y. D., Bec, B., Sautour, B., Froidefond, J. M., Gohin, F., Maurer, D., Plus, M., Laborde, P., and Chardy, P.: Typology of environmental conditions at the onset of winter phytoplankton blooms in a shallow macrotidal coastal ecosystem, Arcachon Bay (France), J. Plankton Res., 29, 999–1014, 2007.

Glé C., Amo, Y. D., Sautour, B., Laborde, P., and Chardy, P.: Variability of nutrients and phytoplankton primary production in a shallow macrotidal coastal ecosystem Arcachon Bay, France. Estuarine, Coast. Shelf Sci., 76, 642–656, 2008.

Goto, N., Mitamura, O., and Terai, H.: Biodegradation of photosynthetically produced extracellular organic carbon from intertidal benthic algae, J. Exp. Mar. Biol. Ecol., 257, 73–86, 2001.

Green, M. A., Jones, M. E., Boudreau, C. L., Moore, R. L., and Westman, B. A.: Dissolution mortality of juvenile bivalves in coastal marine deposits, Limonol. Oceanogr., 49, 727–734, 2004.

Guarini, J. M.: Modélisation de la dynamique du microphytobenthos des vasières intertidales du bassin de Marennes-Oléron, PhD Thesis, Université Pierre et Marie Curie, 177 pp., 1998.

Guo, H., Noormets, A., Zhao, B., Chen, J., Sun, G., Gu, Y., Li, B., and Chen, J.: Tidal effects on net ecosystem exchange of carbon in an estuarine wetland, Agr. Forest Meteorol., 149, 1820–1828, 2009.

Houghton, R. A. and Woodwell, G. M.: The Flax Pond ecosystem study: exchanges of CO_2 between a salt marsh and the atmosphere, Ecology, 61, 1434–1445, 1980.

Hsieh, C. I., Katul, G., and Chi, T. W.: An approximate analytical model for footprint estimation of scalar fluxes in thermally stratified atmospheric flows, Adv. Water Res., 23, 765–772, 2000.

Hubas, C., Davoult, D., Cariou, T., and Artigas, L. P.: Factors controlling benthic metabolism during low tide along a granulometric gradient in an intertidal bay (Roscoff Aber Bay, France), Mar. Ecol. Prog. Ser., 316, 53–68, 2006.

Kaimal, J. C., Wyngaard, J. C., Izumi, Y., and Cote, O. R.: Spectral characteristics of surface layer turbulence, Q. J. Roy. Meteorol. Soc., 98, 563–589, 1972.

Kathilankal, J. C., Mozdzer, T. J., Fuentes, D., D'Odorico, P., McGlathery, K. J., and Zieman, J. C.: Tidal influences on carbon assimilation by a salt marsh, Environ. Res. Lett., 3, 1–6, 2008.

Laruelle, G. G, Dürr, H. H., Slomp, C. P., and Borges, A. V.: Evaluation of sinks and sources of CO_2 in the global coastal ocean using a spatially-explicit typology of estuaries and continental shelves, Geophys. Res. Lett., 37, L15607, doi:10.1029/2010GL043691, 2010.

Leclerc, M. Y. and Thurtell, G. W.: Footprint prediction of scalar fluxes using a Markovian analysis, Bound.-Lay. Meteorol., 52, 247–258, 1990.

Leuschner, C., Landwehr, S., and Mehlig, U.: Limitation of carbon assimilation of intertidal *Zostera noltii* and *Zostera marina* by dessication at low tide, Aquatic Botany, 62, 171–176, 1998.

Mantoura, R. F. C., Martin, J. M., and Wollast, R.: Ocean margin processes, in Global Change, Chichester, UK: Wiley & Sons, 469 pp., 1991.

Middelburg, J. J., Barranguet, C., Boschker, H. T. S., Hermann, P. M. J., Moens, T., and Heip, C. H. R.: The fate of intertidal microphytobenthos carbon: an *in situ* ^{13}C-labeling study, Limnol. Oceanogr. 45, 1224–1234, 2000.

Migné, A., Davoult, D., Spilmont, N., Boucher, G., Gattuso, J. P., and Rybarczyk, H.: A closed-chamber CO_2 flux method for estimating primary production and respiration under emersed conditions, Mar. Biol., 140, 865–869, 2002.

Migné, A., Spilmont, N., and Davoult, D.: *In situ* measurements of benthic primary production during emersion: seasonal variations and annual production in the Bay of Somme (eastern English Channel, France), Cont. Shelf Res., 24, 1437–1449, 2004.

Migné, A., Gévaert, F., Créach, A., Spilmont, N., Chevalier, E., and Davoult, D.: Photosynthetic activity of intertidal microphytobenthic communities during emersion : in situ measurements of Chlorophyll fluorescence (PAM) and CO_2 flux (IRGA), J. Phycol., 43, 864–873, 2007.

Moncrieff, J.-B., Massheder, J. M., de Bruin, H., Elbers, J., Friborg, T., Heusinkveld, B., Kabat, P., Scott, S., Soegaard, H., and Verhoef, A.: A system to measure surface fluxes of momentum, sensible heat, water vapour and carbon dioxide, J. Hydrol., 188–189, 589–611, 1997.

Moore, C. J.: Frequency response corrections for eddy correlation systems, Bound. Lay. Meteorol., 37, 17–35, 1986.

Morison, J. I. L., Piedade, M. T. F, Müller, E., Long, S. P., Junk, W. J., and Jones, M. B.: Very high productivity of the C_4 aquatic grass *Echinochloa polystachya* in the Amazon floodplain confirmed by net ecosystem CO_2 flux measurements, Oecologia, 125, 400–411, 2000.

Odum, H. T.: Primary production in flowing waters, Limnol. Oceanogr., 1, 102–117, 1956.

Ouisse, V., Migne, A., and Davoult, D.: Seasonal variations of community production, respiration and biomass of different primary producers in an intertidal *Zostera noltii* bed (Western English Channel, France), Hydrobiologia, 649, 3–11, 2010.

Parsons, T. R., Takahashi, M., and Hargrave, B.: Biological Oceanographic Processes, 3^{rd} edn. Pergamon Press Ltd, Oxford, 330 pp., 1984.

Pernetta, J. C and Milliman, J. D.: Land-Ocean interactions in the coastal zone. Implementation plan, IGPB Rep., 33, 1–215, 1995.

Plus, M., Stanisière, J.-Y., Maurer, D., and Dumas, F.: Etude comparative des composantes hydrodynamiques de deux systèmes côtiers mésotidaux, les Bassins d'Arcachon et de Marennes-Oléron, Rapport commun LER-AR/LER-PC/DYNECO PHYSED, Ifremer, 1–25, 2008.

Plus, M., Dalloyau, S., Trut, G., Auby, I., de Montaudouin, X., Emery, E., Noël, C., and Viala, C.: Long-term evolution (1988–2008) of *Zostera* spp. Meadows in Arcachon bay (Bay of Biscay), Estuarine, Coast. Shelf Sci., 87, 357–366, 2010.

Raymond, P. A. and Cole, J. J.: Gas exchange in rivers and estuaries: choosing a gas transfer velocity, Estuaries, 24, 312–317, 2001.

Rimmelin, P., Dumon, J. C., Maneux, E., and Gonçalves, A.: Study

of annual and seasonal dissolved inorganic nitrogen inputs into the Arcachon flat, Atlantic coast France, Estuarine, Coast. Shelf Sci., 47, 649–659, 1998.

Rocha, A. V. and Goulden, M. L.: Large interannual CO_2 and energy exchange variability in a freshwater marsh under consistent environmental conditions, J. Geophys. Res., 113, G04019, 1–12, 2008.

Serôdio, J., Vieira, S., and Cruz, S.: Photosynthetic activity, photoprotection and photoinhibition in intertidal microphytobenthos as studied in situ using variable chlorophyll fluorescence, Cont. Shelf Res., 28, 1363–1375, 2008.

Silva, J., Santos, R., Calleja, M. Ll., and Duarte, C. M.: Submerged versus air-exposed intertidal macrophyte productivity: from physiological to community-level assessments, J. Exp. Mar. Biol. Ecol., 317, 87–95, 2005.

Silva, J., Feijo, P., and Santos, R.: Underwater measurements of carbon dioxide evolution in marine plant communities: A new method, Estuar. Coast. Shelf Sci., 78, 827–830, 2008.

Silva, J. and Santos, R.: Reply to comments of G. Abril on "Underwater measurements of carbon dioxide evolution in marine plant communities: A new method" by J. Silva and R. Santos [Estuarine, Coast. Shelf Sci. 78(2008) 827–830], Estuarine, Coast. Shelf Sci., 82, 361–362, 2009.

Smith, S. V. and Hollibaugh, J. T.: Coastal metabolism and the ocean organic carbon balance, Rev. Geophys., 31, 75–89, 1993.

Spilmont, N., Davoult, D., and Migné, A.: Benthic primary production during emersion: in situ measurements and potential primary production in the Seine Estuary (English Channel, France), Mar. Pollut. Bull., 54, 49–55, 2006.

Vachon, D., Prairie, Y. T., and Cole, J. J.: The relationship between near-surface turbulence and gas transfer velocity in freshwater systems and its effect on floating chamber measurements, Limnol. Oceanogr., 55, 1723–1732, 2010.

Yan, Y., Zhao, B., Chen, J., Guo, H., Gu, Y., Wu, Q., and Li, B.: Closing the carbon budget of estuarine wetlands with tower-based measurements and MODIS time series, Glob. Change Biol., 14, 1690–1702, doi:10.1111/j.1365-2486.2008.01589.x, 2008.

Wang, Z. A. and Cai, W.-J.: Carbon dioxide degassing and inorganic carbon export from a marsh-dominated estuary (the Dublin River): a marsh CO_2 pump, Limnol. Oceanogr., 49, 341–354, 2004.

Ware, J. R., Smith, S. V., and Reaka-Kudla, M. L.: Coral reefs: sources or sinks of atmospheric CO_2?, Coral Reefs, 11, 127–130, 1991.

Webb, E. K., Pearman, G., and Leuning, R.: Correction of flux measurements for density effects due to heat and water vapour transfer, Q. J. Roy. Meteorol. Soc., 106, 85–100, 1980.

Zemmelink, H. J., Slagter, H. A., van Slooten, C., Snoek, J., Heusinkveld, B., Elbers, J., Bink, N. J., Klaassen, W., Philippart, C. J. M., and de Baar, H. J. W.: Primary production and eddy correlation measurements of CO_2 exchange over an intertidal estuary, Geophys. Res. Lett., 36, LI19606, doi:10.1029/2009GL039285, 2009.